Where should sports events be held under global warming? A case study of the African Cup of Nations

Windmanagda Sawadogo, Jan Bliefernicht, Aissatou Faye, Harald Kunstmann

Angaben zur Veröffentlichung / Publication details:

Sawadogo, Windmanagda, Jan Bliefernicht, Aissatou Faye, and Harald Kunstmann. 2025. "Where should sports events be held under global warming? A case study of the African Cup of Nations." *Sustainable Cities and Society* 119: 106091. https://doi.org/10.1016/j.scs.2024.106091.

Sustainable Cities and Society 119 (2025) 106091

Contents lists available at ScienceDirect

Sustainable Cities and Society

journal homepage: www.elsevier.com/locate/scs

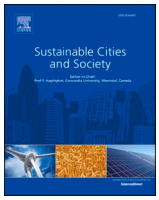

Where should sports events be held under global warming? A case study of the African Cup of Nations

Windmanagda Sawadogo [a,*], Jan Bliefernicht [a], Aissatou Faye [b], Harald Kunstmann [a,c,d]

[a] Institute of Geography, University of Augsburg, 86159 Augsburg, Germany
[b] Department of Environmental Sciences, University of Virginia, Charlottesville, VA 22904, USA
[c] Center for Climate Resilience, University of Augsburg, 86159 Augsburg, Germany
[d] Institute of Meteorology and Climate Research (IMK-IFU), Karlsruhe Institute of Technology (KIT), Campus Alpin, 82467, Garmisch-Partenkirchen, Germany

ARTICLE INFO

Keywords:
Climate change
CMIP6
Wet-bulb globe temperature
Heat stress
Football
Afcon
Sustainability
Africa

ABSTRACT

Africa is a global hotspot for climate change, affecting various sectors, including sports. Against this backdrop, major international sports events such as the African Cup of Nations (Afcon) could become more complex under global warming. This study examines projected changes in the wet-bulb globe temperature (WBGT) index used as a proxy to determine suitable Afcon host countries under climate change conditions. Using eleven CMIP6 simulations from NASA's NEX-GDDP-CMIP6, downscaled to a 25 km resolution, the analysis covers three shared socioeconomic pathways (SSP1–2.6, SSP2–4.5, and SSP5–8.5) climate change scenarios for the near future (2031–2060) and far future (2071–2100), relative to 1985–2014. The model ensemble mean reproduced the spatial distribution of the WBGT index and related variables well with the reference datasets over Africa but with some biases. Projections indicate a significant WBGT increase across Africa under all scenarios and periods, especially under SSP5–8.5 in the far future, with a value of about 6 °C. Many countries may transition from an unrestricted to a high-risk status. Climate change could notably reduce the number of Afcon host countries under the SSP5–8.5 scenario. This study provides valuable insights for Afcon hosting and climate change integration, contributing to resilience and sustainability in urban environments hosting such events.

1. Introduction

Climate change threatens human beings and has become a state affair. According to the United Nations Framework Convention on Climate Change, human activities inducing warming, are the main cause of climate change (UNFCCC, 1992). The effects of climate change are numerous in all countries and contribute to the loss of life, damage, and a decline in population well-being (Nyiwul, 2021; Ebi et al., 2021; Warner & van der Geest, 2013). The Paris Agreement proved the awareness of policymakers, stakeholders, and governments to lower our carbon footprint to reduce the Earth's global mean temperature to 2 °C and further to 1.5 °C (Maslin et al., 2023). To achieve this goal, we need to reduce our greenhouse gas emissions. This is one of the key recommendations of the conference of parties held in Dubai in 2023 to achieve net-zero emissions by 2050 (Locke et al., 2023). Nonetheless, we are still currently facing severe impacts from climate change, and February 2024 is the warmest February ever recorded (ECMWF, 2024). Exposure to high outdoor temperatures is associated with morbidity and an increased risk of premature death (Vicedo-Cabrera et al., 2021). Therefore, the impacts of climate change may put outdoor activities such as football in danger.

Football has gained popularity in recent years and has become the favorite sport in Africa. The *Confédération Africaine de Football* (CAF) is a confederation that attributes and organizes the prestigious tournament of the continent: the African Cup of Nations (Afcon). The latest Afcon (Afcon-2023) was held in Côte d'Ivoire from mid-January to mid-February 2024. Three games were played during the tournament's group stages, and two were played in the other phases, leading up to the final. In the group stages, the games were played at 14:00, 17:00 and 20:00 GMT; in the latter stage, two games were played at 17:00 and 20:00 GMT. Due to the high temperature and humidity in Côte d'Ivoire, the players had two-minute rest and refreshing breaks in the 30th minute in the first half and the 75th minute in the second period, following the recommendation of Fédération Internationale de Football Association (FIFA). According to the CAF regulations, the temperature and relative humidity are measured before the kick-off to ensure the

* Corresponding author.
E-mail address: windmanagda.sawadogo@uni-a.de (W. Sawadogo).

https://doi.org/10.1016/j.scs.2024.106091
Received 8 August 2024; Received in revised form 16 December 2024; Accepted 17 December 2024
Available online 18 December 2024

players' performance and to diagnose and treat heat-related illnesses (CAF, 2024). Several studies have shown that football players' performance significantly decreases during games under high temperature and humidity conditions (Gibson et al., 2019; Racinais et al., 2015; Mohr et al., 2012; Grantham et al., 2010).

High temperatures are expected to increase over the African continent by 4.4 °C, with the highest warming of 5.6 °C occurring in the Sahel region and the lowest warming of 3.5 °C occurring in Central Africa under the shared socioeconomic pathway (SSP) 5–8.5 (Almazroui et al., 2020). Climate change is likely to amplify the intensity of hot days and nights by 1.5–3 °C and 1–4 °C, respectively, in Africa under SSP scenarios (Das et al., 2023). Sawadogo et al. (2024) reported increased temperature and heat stress days across Burkina Faso under SSP scenarios. On the other hand, the effect of increasing temperature on human comfort is expected to be significant. For instance, Fotso-Nguemo et al. (2023) showed that heat stress categories susceptible to creating discomfort for populations are likely to increase in Africa. However, this discomfort is not uniform across Africa and some regions will likely face higher risk than others. This is the case in the West African region, particularly in the Sahel region, where most of these countries will experience more than a 50 % increase in heat stress days due to global warming (Sylla et al., 2018). Heat stress may also contribute to a decline in player performance in a football game (Ozgünen et al., 2010). Given these projections and the potential impacts of heat stress on human discomfort and performance, incorporating indices such as the wet bulb globe temperature (WBGT) has become paramount (Mahgoub et al., 2020; Kakaei et al., 2019).

The WBGT index is an international standard for measuring the effect of heat-related stress on the human body. This index is more comprehensive and tailored for outdoor conditions under direct sunlight. This makes it a valuable metric for assessing the thermal conditions faced by individuals working outdoors and athletes (Spangler et al., 2022). For instance, Chowdhury et al. (2017) identified June and July months as high health risk factors in workplaces in Dhaka, Bangladesh, based on WBGT analysis. Over the last decades, South Asia has experienced a significant increase in WBGT during monsoon and pre-monsoon periods, exposing the population to extreme heat (Kyaw et al., 2023).

On the other hand, the WBGT is also used to determine the heat stress of players in football (FIFA, 2015). A study by Nassis et al. (2015) investigated the impact of hot environmental conditions on football players during the 2014 FIFA World Cup in Brazil using the WBGT index. Their study revealed that high-intensity activity and the number of sprints during a game were reduced at high WBGT values. In Germany, Chmura et al. (2021) found that a high WBGT affects players' total distance covered and sprint performance during five consecutive Bundesliga seasons. This is also true among female football players (Austin et al., 2021). With the decrease in player performance at high WBGT levels, some researchers have investigated the impacts of global warming on the WBGT index. For instance, Newth and Gunasekera (2018) found an increase in WBGT under RCP2.6 (0.6–1.7 °C) and RCP8.5 (2.37–4.4 °C) globally. Compared with the 1961–1990 reference period, Brazil is likely to expect an increase in the WBGT under global warming (Bitencourt et al., 2021). A restricted continuous physical activity level is likely to be reached under the RCP8.5 scenario in Australia (Hall et al., 2022). In Eastern Africa, Yengoh and Ardö (2020) projected an increase in WBGT in Kenya and Tanzania that could affect smallholder farmers' rest and work cycles.

Despite previous studies on the impact of climate change on heat-related stress, there is a notable gap in the literature on how projected changes in heat stress, as measured by the WBGT, might affect major sports events in Africa. While studies have examined the WBGT in relation to health safety and exercise-induced heat stress in Africa (Raines & Fitchett, 2024; Brimicombe et al., 2024), no study to date has systematically examined the future impact of climate change on the suitability of African countries to host major tournaments such as the Afcon. This gap is significant as Africa is a climate change hotspot and Afcon is one of the continent's most important international sporting events. Our study addresses this unexplored interface between climate change, football, and sports event planning by using the WBGT index as a proxy to assess how global warming will constrain or limit host countries under different climate scenarios. Moreover, the study is the first to combine climate projections with a comprehensive analysis of the WBGT index to assess future risks for hosting sports events, which provides critical insights for decision-making under global warming conditions for sustainable societies.

To achieve that, we used eleven Coupled Model Intercomparison Project Phase 6 (CMIP6) datasets from NASA Earth Exchange Global Daily Downscaled Projections (NEX-GDDP-CMIP6), statistically downscaled to a spatial resolution of 25 km. Future changes in the WBGT are carried out under three SSPs: SSP1–2.6, SSP2–4.5, and SSP5–8.5. We projected the WBGT for the near-future period (2031–2060) and the far-future period (2071–2100) relative to the 1985–2014 baseline period. Furthermore, we used the WBGT index as a proxy to identify suitable countries in the near and far future under the SSP scenarios to host the Afcon based on the different alert status categories. The induced changes in the WBGT relative to the air temperature (*tas*), relative humidity (*hurs*), and surface downwelling shortwave radiation (*rsds*) are also investigated. We also quantified the uncertainties related to the increase in WBGT in Africa and its subregions. The results of this study can serve as a benchmark for policymakers, and the CAF to consider global warming as a factor for selecting appropriate months for the selected countries.

The paper is structured as follows: Section 2 highlights the study area, data, and methods used in this study, while Section 3 presents the results and discussion section. Finally, Section 4 presents the conclusion of the study.

2. Materials and methods

2.1. Climate and reference datasets

We used datasets from NEX-GDDP-CMIP6 to project future changes in the WBGT in Africa. Several studies have used the NEX-GDDP-CMIP6 dataset for climate impact studies (Sawadogo et al., 2024; Rao et al., 2024; Airiken et al., 2023). These datasets are statistically downscaled climate scenarios derived from CMIP6 models to a horizontal resolution of 0.25° with a bias correction and spatial disaggregation (BCSD) method (Thrasher et al., 2022). The latest version of Global Meteorological Forcing Dataset (GMFD) for Land Surface Modeling was used as a reference for the bias correction of different CMIP6 simulations. NEX-GDDP-CMIP6 encompasses 35 climate models and five experiments: historical, SSP1–2.6, SSP2–4.5, SSP3–7.0, and SSP5–8.5. The historical period spans from 1960 to 2014, while the future period ranges from 2015 to 2100. In addition, only the r1i1p1f1 variant was used in NEX-GDDP-CMIP6, which included nine variables: relative and specific humidity, precipitation, surface downwelling longwave and shortwave radiation, surface wind speed, minimum, maximum, and mean temperature. For this study, we selected eleven climate models based on variable availability (*hurs, rsds*, and *tas*) and scenarios (SSP1–2.6, SSP2–4.5, and SSP5–8.5). The different models used in this study are listed in Table.S1 (see supplementary material).

For the reference data, we used two datasets. The first dataset comes from the European Centre for Medium-Range Weather Forecasts (ECMWF) reanalysis dataset, version 5 (ERA5; Hersbach et al., 2020).

ERA5 is the fifth-generation ECMWF atmospheric global climate reanalysis with a spatial resolution of 31 km. It covers the period from January 1940 to the present and has 37 pressure levels from 1000 (surface) to 1 hPa. We downloaded the *hurs* and *tas* variables from 1985 to 2014. Note that *hurs* is not an available straightforward variable in ERA5; *hurs* is computed from tas and dewpoint temperature following the equation given in Alduchov and Eskridge (1996).

The second dataset is sourced from the CM SAF third edition of the Surface Solar Radiation Data Set-Heliosat (SARAH-3; Pfeifroth et al., 2023). SARAH-3 is a satellite-based climate data record from 1981 to the present with a lag of two days. It has a spatial resolution of approximately 5 km and covers the region at ±65° longitude and ±65° latitude. We retrieved daily *rsds* data from 1985 to 2014.

2.2. Wet-bulb globe temperature

The WBGT is defined as the measure of heat stress in direct sunlight. It was originally developed in the 1950s to ensure safety and avoid heat illnesses at US military camps (Budd, 2008). The WBGT index is a suitable heat index for evaluating working environment conditions due to its capacity to assess heat exposure effects over time and its ease of use (Kakaei et al., 2019). In recent decades, the WBGT has been widely used in sports such as football to assess players' performance and/or the recommendation to cancel a game or not (Tripp et al., 2020). In this study, we use the WBGT index, which is computed daily, to assess the suitable countries to host Afcon under climate change conditions. Following Parsons (2006), for outdoor environments with solar radiation, the WGBT can be expressed as:

$$WBGT = 0.7 \times T_w + 0.2 \times T_g + 0.1 \times tas \tag{1}$$

where T_w is the natural wet temperature, T_g is the black globe temperature, and *tas* is the air temperature.

Since T_w and T_g are not recorded by weather stations or climate model outputs, we need to find another way to estimate them. Stull (2011) proposed an analytical psychrometric equation to calculate T_w as a function of *hurs* and *tas* at standard sea level pressure with a mean deviation of less than 0.3 °C. T_w is expressed as:

$$T_w = tas \times arctan\left[0.15977 \times (hurs + 8.313659)^{0.5}\right] + arctan(tas + hurs) - arctan(hurs + 1.676331) + 0.00391838 \times hurs^{3/2} * arctan(0.023101 \times hurs) - 4.686035 \tag{2}$$

To compute T_g, we used the results from Hajizadeh et al. (2017), where T_g is estimated using a linear regression model with a significant correlation coefficient of 0.95. It can be estimated as:

$$T_g = 0.01498 \times rsds + 1.184 \times tas - 0.0789 \times hurs - 2.739 \tag{3}$$

We classified the obtained values of the WBGT from Eq. (1). Following Zare et al.(2018); Brocherie and Millet (2015), Table 1 summarizes the classification of the WBGT index values, their alerts, and recommended sports activities.

2.3. Climate change analysis

This study focuses on the African continent, its subregions, and different countries (Fig. 1). The first analysis involves assessing the climate model with reference data. This exercise is necessary to ensure the ability of climate models to reproduce the spatial pattern of the reference data used in this study. All the reference data are interpolated to the spatial resolution of the NEX-GDDP-CMIP6 dataset via the bilinear grid interpolation technique. Some statistical metrics, such as spatial correlation (R), mean bias error (MBE), and overall performance (OP), are also used for model evaluation. The OP is a new statistical metric introduced by Sawadogo et al. (2023), combining the normalized root-mean-square-error (nRMSE), correlation R, and index of agreement (IOA), and it is expressed as:

$$OP = 1 - \left(\frac{nRMSE}{100} + (1 - R) + (1 - IOA)\right) \tag{4}$$

The OP is dimensionless. +1 means that the model is perfectly close to the reference data, while a negative value indicates that the model is far from the reference data. The IOA is defined as:

$$IOA = 1 - \frac{\sum_{i=1}^{n}(P_i - O_i)}{\sum_{i=1}^{n}(|P_i - \overline{O}||O_i - \overline{O}|)^2} \tag{5}$$

where P is EnsMean, O the Ref data. $\overline{O}$ is the mean value of the Ref data.

The projected changes in the WBGT index are determined under three SSP climate scenarios. SSPs are narrative scenarios for the future development of human societies. These factors include demographics (population growth), inequality, human development, technological change, economic growth, governance, and policy orientations. The SSP scenarios have five socioeconomic families and are classified into two major groups: challenges to mitigation and challenges to adaptation (O'Neill et al., 2014). These new climate scenarios do not replace the RCP scenarios but rather expand them (O'Neill et al., 2020).

This study selected three socioeconomic families (SSP1, SSP2, and SSP5) associated with three radiative forcings (2.6, 4.5, and 8.5 W m^{-2}, respectively). SSP1–2.6 describes one of the most optimistic scenarios of the Intergovernmental Panel on Climate Change (IPCC), aiming to reach net zero emissions before 2050. Moreover, it also aims to stabilize the global mean temperature (GMT) by 1.8 °C at the end of the century, aligning with the target of the Paris Agreement. On the other hand, in the SSP5–8.5 scenario, the GMT could increase to 4.4 °C by 2100, as twofold greater CO_2 emission levels than our current emissions are expected by 2050. This scenario is classified as the worst-case scenario among the SSP scenarios. Between the two extreme scenarios, we also selected the SSP2–4.5 scenario. This scenario represents the "middle of the road," and the GMT could increase to 2.7 °C by the end of the century. These selected SSP scenarios provide a broad overview of the

Table 1
Recommended WBGT index values for outdoor activities and their implications.

WBGT (°C)	Thermal sensation	Alert description	Recommended sport activity
< 18	Neutral	Unrestricted	Unlimited
18 - 24	Warm	Low-risk	Remain vigilant for potential index rises and signs of heat stress
24 - 28	Hot	High-risk	Reduce physical activity for individuals who are not acclimatized
28 –30	Very hot	Very high-risk	Limit physical activity for individuals who are not well-acclimated
> 30	Sweltering	Stop-play	All training should be stopped

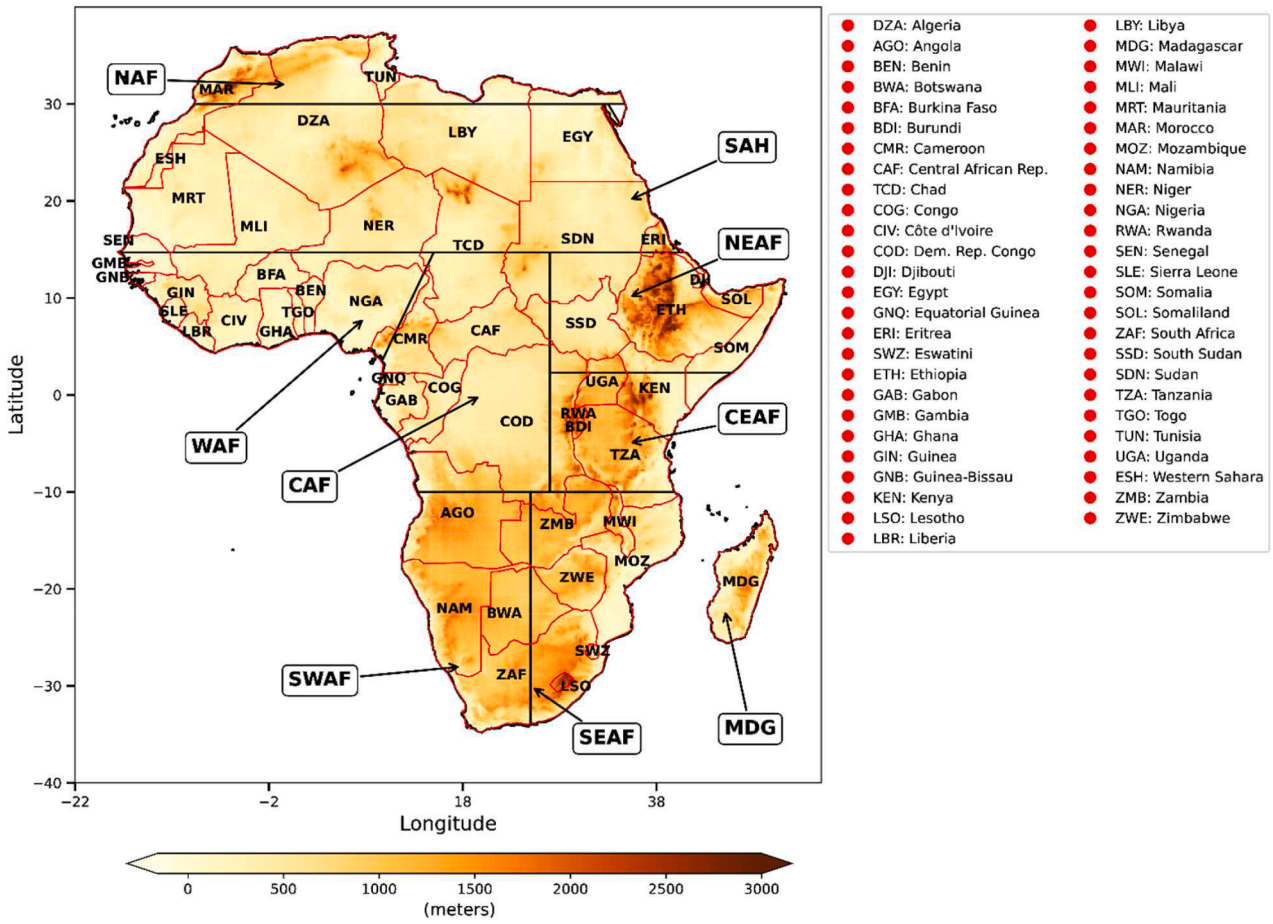

Fig. 1. Study area showing the topography. Each label in the box indicates a subregion. NAF: North Africa; SAH: Sahara; WAF: West Africa; CAF: Central Africa; NEAF: North-East Africa; CEAF: Central-East Africa; SWAF: South-West Africa; SEAF: South-East Africa and MDG: Madagascar. The borders of the countries are depicted in red lines with their code name. The meaning of the code names is presented on the right side as a red circle.

impacts of climate change on the WBGT index in Africa under the optimistic, worst, and intermediate scenarios.

The projected changes in the WBGT index and all related variables are in absolute terms. Two future periods were considered: the near future (2031–2060) and the far future (2071–2100) relative to the reference period of 1985–2014. All the analyses used the arithmetic multimodel ensemble mean (hereafter, *EnsMean*) of the NEX-GDDP-CMIP6. The robustness of the climate signal change is analyzed following Fischer et al. (2014), where 80 % of the simulations agree in the same direction. Additionally, we employed a *t*-test, using a 95 % confidence interval, to evaluate the significance of the change, which is indicated as a dot for each grid point. We used the monthly and annual daily means of the WBGT for the climate change projections. Finally, the suitable countries based on the WBGT index are identified by projecting the changes in alert descriptions stated in Table 1. This is provided by taking the 75th percentile of grid points within each country in the reference and future change periods. The change in the alert description is the sum of the future change period and the reference for the respective countries, and then it is normalized to the alert description. The change in alert description is carried out on a monthly and annual mean scale.

2.4. Induced changes in the WBGT

To understand the relative importance of the different variables in calculating the WBGT index under climate change, we computed the induced change in the WBGT. This is calculated by substituting the T_w and T_g expressions into Eq. (1). *rsds, hurs*, and *tas* are the main variables contributing to the change in the WBGT. We used a method similar to that used by Sawadogo et al. (2019); Jerez et al. (2015) to isolate different variables, which can be expressed as:

$$\Delta WBGT = \Delta tas_{WBGT} + \Delta hurs_{WBGT} + \Delta rsds_{WBGT} \tag{6}$$

where Δtas_{WBGT}, $\Delta hurs_{WBGT}$ and $\Delta rsds_{WBGT}$ are the contributions to the total change in the WBGT.

Following the first order of Taylor approximation, Δtas_{WBGT} and $\Delta rsds_{WBGT}$ can be expressed as:

$$\Delta tas_{WBGT} = \Delta tas \times 0.7 \times \left\{ arctan\left[0.151977 \times (hurs + 8.3313659)^{0.5}\right] + \frac{1}{1 + (hurs + tas)^{2}} \right\} + 0.3368 \tag{7}$$

$$\Delta rsds_{WBGT} = \Delta rsds \times 0.002996 \quad (8)$$

From Eq. (6), we can deduce that:

$$\Delta hurs_{WBGT} = \Delta WBGT - \Delta hurs_{WBGT} - \Delta rsds_{WBGT} \quad (9)$$

The contribution changes are given in relative terms by dividing Eqs. (7), (8) and (9) by $\Delta WBGT$.

2.5. Uncertainty analysis

To support robust decision-making and risk management related to climate change impacts, we quantified uncertainties in projecting changes in the WBGT across the NEX-GDDP-CMIP6 datasets used in this study. Following the methodology of Hawkins and Sutton (2009), the source of uncertainties is partitioned into three sources: internal variability (V), model uncertainty (M), and scenario uncertainty (S). All the NEX-GDDP-CMIP6 data under the different scenarios are fitted using ordinary least squares with a fourth-order polynomial from 1960 to 2100. The raw prediction X for each model can be written as:

$$X_{m,s,t} = x_{m,s,t} + i_{m,s} + \varepsilon_{m,s,t} \quad (10)$$

where m, s, and t indicate the model, scenario, and year, respectively. $x_{m,s,t}$ represents the smooth fit of the fourth-order polynomial, $i_{m,s}$ denotes the multiyear average WBGT of the 1985–2014 period and $\varepsilon_{m,s,t}$ indicates the residuals of the fitted equation.

The internal variability (V) is defined as the average variance of the multimodel residuals, and it is written as:

$$V = \frac{1}{N_m}\sum_{m} var_{s,t}(\varepsilon_{m,s,t}) \quad (12)$$

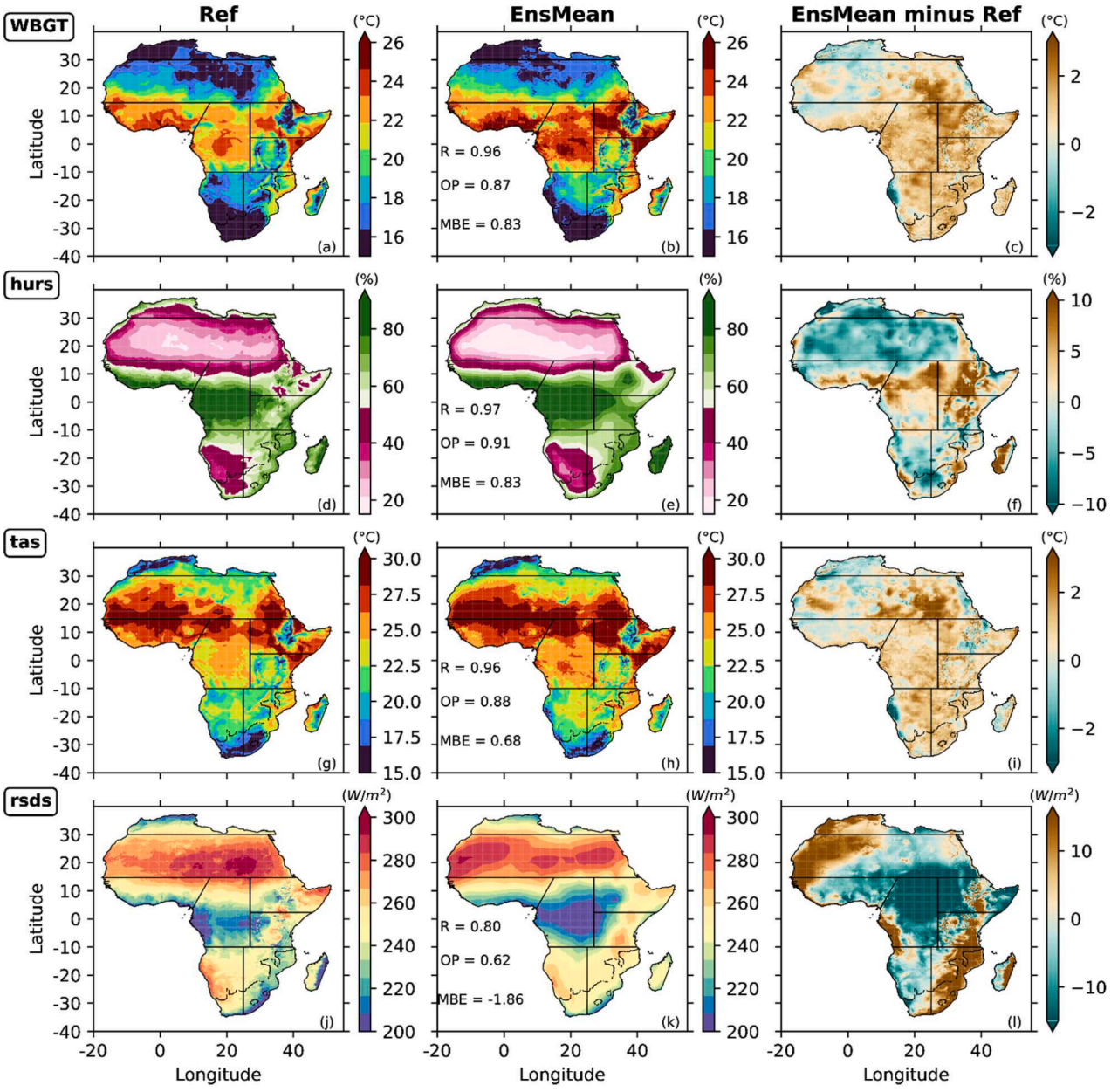

Fig. 2. Mean annual spatial distribution of the daily wet bulb globe temperature (WBGT), relative humidity (*hurs*), air temperature (*tas*), and shortwave radiation (*rsds*) for the reference data (*Ref*) and the multimodel ensemble mean of the NEX-GDDP-CMIP6 (*EnsMean*) with their bias (*EnsMean* minus *Ref*) in the present climate (1985–2014). Each row shows the variables, while the column indicates the name of the data. R indicates the spatial correlation. OP represents the overall spatial performance and the mean absolute error, respectively.

where $var_{s,t}$ is the variance across scenarios and years, V is constant over time, and N_m is the number of models used.

The model uncertainty (M) for each scenario is calculated based on the weighted variance in the various model prediction fits.

$$M = \frac{1}{N_s}\sum_{m} var_m\left(x_{m,s,t}\right) \tag{13}$$

where N_s is the number of scenarios.

Finally, the scenario uncertainty (S) is defined as the variance of the weighted *EnsMean* for the three scenarios and is calculated as follows:

$$S = var\left(\sum_{m} x_{m,s,t}\right) \tag{14}$$

We hypothesize that the three sources of uncertainties are independent and that the total variance (T) is the sum of the V, M, and S uncertainties:

$$T = V + M + S \tag{15}$$

The sources of uncertainties over Africa and its subregions are represented by the fractional total variance from 2020.

3. Results and discussion

3.1. Model evaluation

The *EnsMean* well captured the spatial annual distribution of the reference data over Africa for the different variables (Fig. 2). The performance of the different variables varies across the continent. The OP values range from 0.62 to 0.91, while the *R* values range from 0.80 to 0.97. The spatial distribution of *hurs* exhibits the highest performance ($OP = 0.91$ and $R = 0.97$), whereas the *rsds* shows the lowest performance ($OP = 0.62$ and $R = 0.80$). *Ref* and *EnsMean* agree on the maximum and minimum spatial distribution in *hurs*. The Sahel and some fringes of the northern regions exhibit the highest values in *hurs* of about 20 %, whereas the central and some areas along the coast of western Africa, south-east Africa, and Madagascar experience high values of approximately 80 %. The lowest values in *hurs* could be explained by the presence of desert, while the highest values could be attributed to the presence of forest or/and the influence of the monsoon system.

High humidity is related to the formation of clouds, which reduce the amount of solar radiation reaching the surface. Conversely, low humidity implies fewer clouds in the atmosphere, leading to clear sky conditions and, thus, more solar radiation at the surface. This is why the maximum values of *rsds* are located in the Saharan region, while the minimum values are in the central African region (Fig. 2j-k). Moreover, *EnsMean* is able to mimic this pattern along with the *Ref* data. Additionally, both datasets converge in the same spatial distribution of *tas* over Africa. They show that the warmer areas are in the Sahelian strip, and the coolest areas are located on the northern edge and at the bottom of Africa (Fig. 2g-h). Similarly, the WBGT index shows the same spatial distribution of *tas* (Fig. 2a-b). We observe similar results between the two datasets, with a high OP of 0.87 and *R* of 0.96. Both datasets exhibit consistent WBGT index gradients at the equator. The annual mean climatology values of the WBGT index range from 15 to 27 °C across the continent and are similar to those found by Kong and Huber (2022) over Africa. Moreover, both datasets agree on the maximum values of the WBGT index, where *hurs* and *tas* are relatively high, and with a low WBGT index, where *hurs* and *tas* are relatively low.

Even with the good performance of *EnsMean* in the spatial distribution of the different variables, there are some notable biases. *EnsMean* indicates an overestimated WBGT index over Africa, with a spatial mean bias of 0.83 °C. The overestimation of the WBGT index could be due to the inherent spatial mean biases observed in *tas* (Fig. 2-i) and *hurs* (Fig. 2-f) of 0.68 °C and 0.83 %, respectively. However, the magnitude of the biases differs from one region to another and among the variables. Near the equator, *EnsMean* overestimates the value of *hurs* by more than 10 %, while in northern Africa, we have an underestimation of approximately 5 %.

In contrast to *hurs, EnsMean* exhibits a general warm bias of *tas* across the regions. Notably, within the Sahel region, localized areas exhibit pronounced warm biases reaching magnitudes as high as 2.5 °C. These high biases could be due to the lack of available radiosonde stations and active land surface stations in these areas for data assimilation in ERA5. The biases in the WBGT are also strong in these localized areas in the Sahel region at approximately 2.0 °C. Apart from these areas, *EnsMean* shows a relatively low bias across Africa in the WBGT index of 1.0 °C. Moreover, *EnsMean* underestimates the *rsds* in central Africa by more than 10 $W.m^{-2}$ and overestimates the *rsds* in Southeast Africa and the eastern part of the Sahel region by more than 10 $W.m^{-2}$. The biases observed in the different variables could be due to the inherent biases from the reference datasets used to statistically downscale the NEX-GDDP-CMIP6 datasets or the reference datasets used to compare the *EnsMean*. Similar biases in tas variables have also been found across

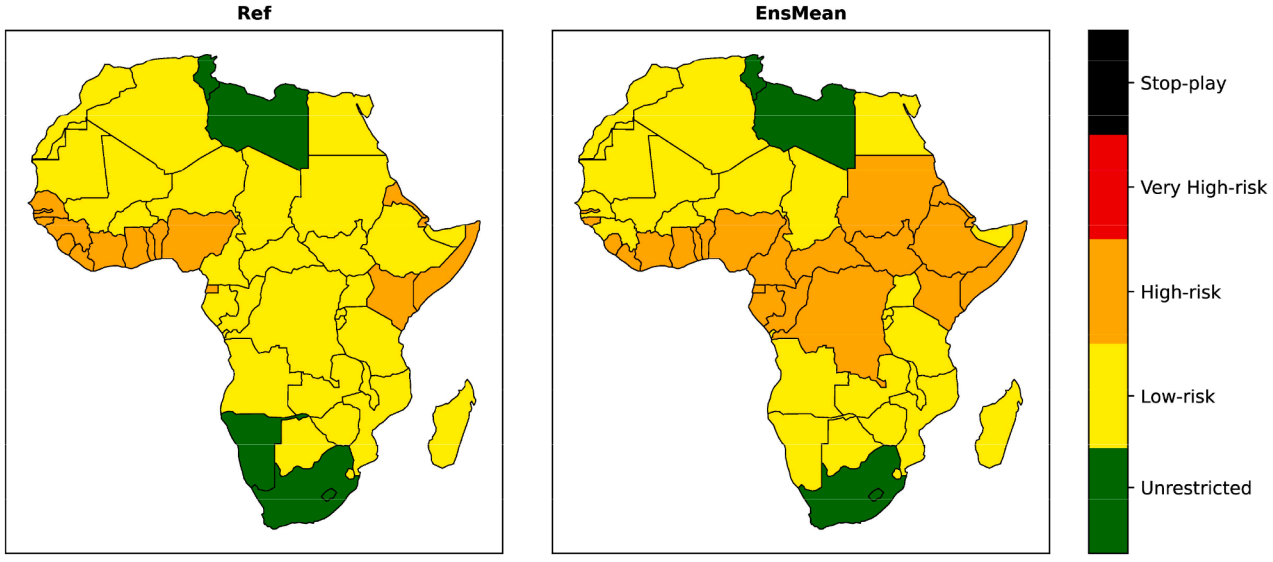

Fig. 3. Annual climatology of the alert description status in the present climate (1985–2014) for the reference data (*Ref*) and the multimodel ensemble mean of the NEX-GDDP-CMIP6 (*EnsMean*). Each color corresponds to a specific alert description status depicted in the color bar.

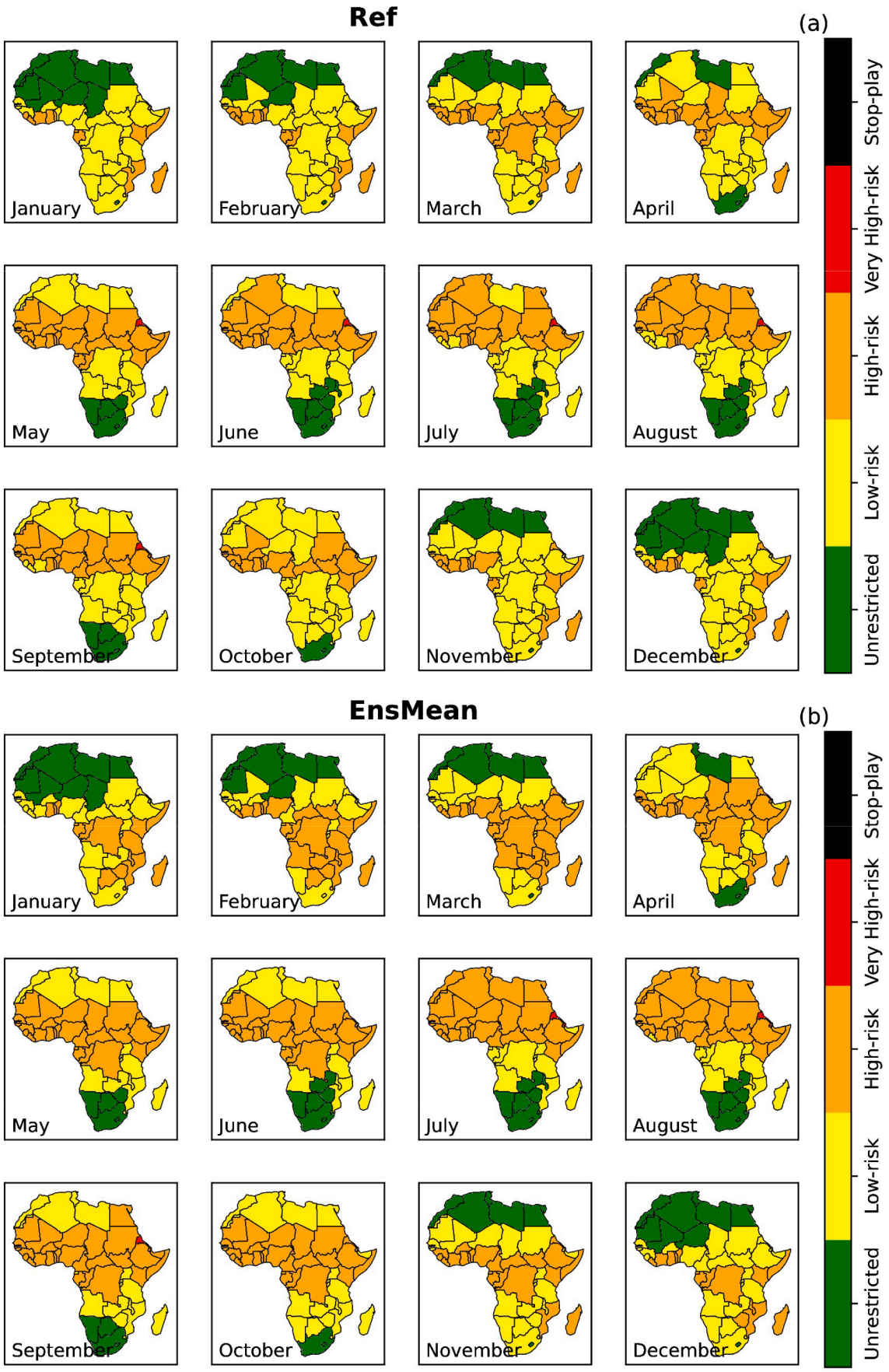

Fig. 4. Similar to Fig. 3 but for monthly climatology.

African regions using CMIP5, CMIP6, or NEX-GDDP-CMIP6 (Sawadogo et al., 2024; Almazroui et al., 2020, 2020). Overall, *EnsMean* shows good performance in reproducing the spatial distributions of the WBGT index, *tas, hurs*, and *rsds*.

Fig. 3 shows the annual climatology of the alert description status for each country based on the WBGT index for the *Ref* and the *EnsMean* datasets in the current climate. Five countries, Libya, Tunisia, South Africa, Namibia, and Lesotho, show an unrestricted alert status under the *Ref* dataset. The *EnsMean* also exhibits a similar unrestricted alert status except for Namibia, where it shows a low-risk alert status. Both datasets agree on the high-risk alert status of coastal countries in West Africa. Most West African countries located in the Sahel region, northern Africa, and some countries in southern Africa indicate a low-risk alert in both datasets. Both datasets disagree on the alert status over central African countries and some countries like Sudan and Ethiopia. This discrepancy is due to the overestimation of the WBGT index over these countries in *EnsMean* (Fig. 2-c). In general, the *Ref* and the *EnsMean* datasets show that most African countries, such as Ghana, Côte d'Ivoire, and Togo, can host the Afcon with some precautions to take due to their high-risk alert status.

However, the alert description status varies throughout the year (Fig. 4). Overall, the *EnsMean* and *Ref* datasets show similar alert description status in most months. There is good agreement between June and September between the two datasets for very high-risk alert status in Eritrea. In addition, there is also a good similarity in the *Ref* and *EnsMean* datasets in January-February and June-July, where most of the Afcon games take place. These months show unrestricted and low-risk alert descriptions in most countries. Countries located above 10° latitude north show an unrestricted alert, and some countries in southern Africa indicate a low-risk alert in January-February, with the situation reversing in June-July. This finding aligns with the climate pattern over the continent, where the January-February and June-July months fall in the winter period in the Northern Hemisphere and Southern Hemisphere, respectively.

3.2. Projected changes in the WBGT index and suitable countries

3.2.1. Projected changes in the WBGT index across Africa

Fig. 5 shows the projection change in annual WBGT under all scenarios and periods over Africa. *EnsMean* projects a significant increase in WBGT across Africa. The projection changes for the two periods suggest that the impacts of climate change on the WBGT will likely become more pronounced in the 2071–2100 period. For instance, under the SSP2–4.5 scenario, an average increase of 1.34 °C is expected for the 2031–2060 period, while an increase of 2.16 °C is expected for the 2071–2100 period. In addition, the SSP5–8.5 scenario exhibits the highest increase, and the SSP1–2.6 scenario indicates the lowest increase in both periods. An average of 3.8 °C and 1.3 °C are projected for the 2071–2100 period under the SSP5–8.5 and SSP1–2.6 scenarios, respectively. These averaged values over the continent fall within the range of projected changes in the WBGT across the globe (Newth & Gunasekera, 2018).

However, these increases are not homogeneous across the continent. Higher increases are observed in the Sahara region and northern and southern Africa, while the lowest increases are observed in central Africa. Under the SSP5–8.5 scenario, some areas of the Sahra region can expect an increase of 5 °C and 4 °C in the southern parts for the 2071–2100 period. These increases could be explained by a similar increase pattern observed in temperature in all scenarios and periods (see supplementary material Fig. S1–2). Moreover, the *EnsMean* project a lower increase in the WBGT in the coastal areas for most scenarios and periods. The projected changes in WBGT exhibit seasonal variation across all scenarios and time periods (see Fig. S3–4). The DJF (December-January-February) and MAM (March-April-May) seasons show a low relative increase compared to the JJA (June-July-August) and SON (September-October-November) seasons. Under the SSP5–8.5 scenario and the 2071–2100 period, there is a significant increase in WBT in some areas of North Africa and the Sahel region of more than 5.0 °C. These differences in WBGT magnitudes among the SSPs illustrate the climate risk of each scenario, highlighting the potential benefits of lower-emission pathways.

These projected changes in the WBGT found in our study are

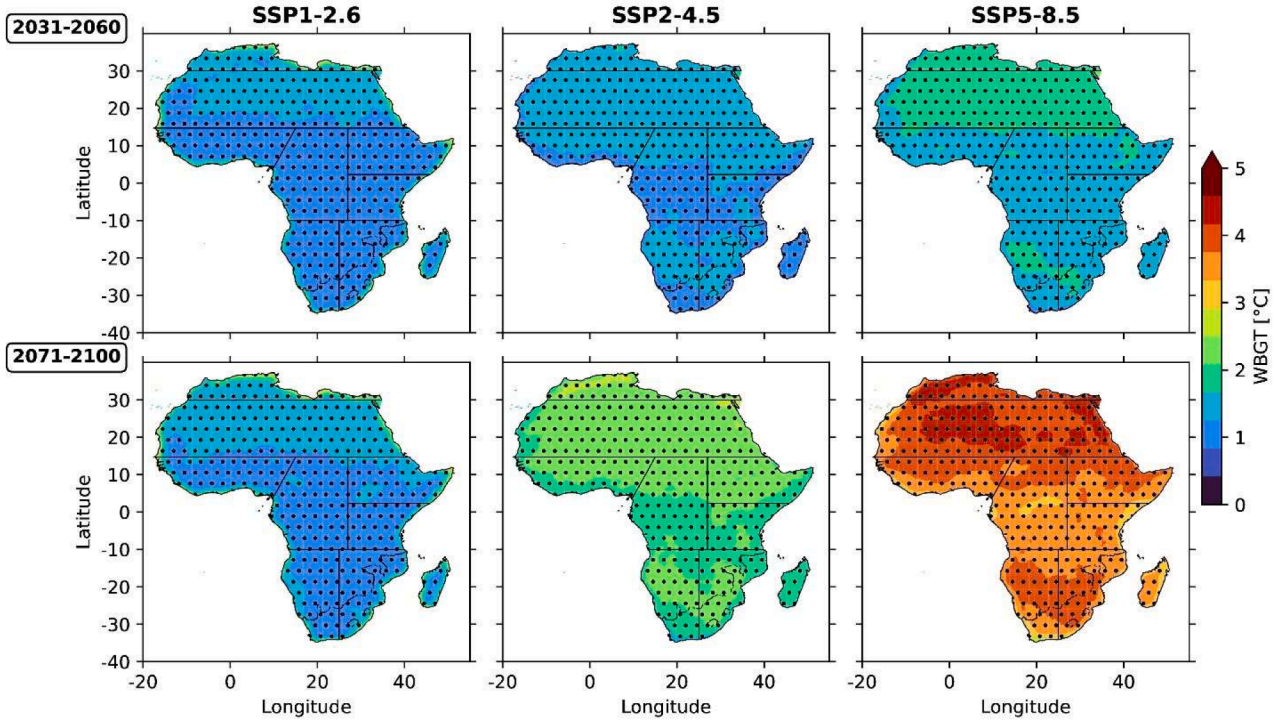

Fig. 5. Annual projected spatial distribution of the WBGT index across Africa of the multimodel ensemble mean of the NEX-GDDP-CMIP6 (*EnsMean*). Each column shows different scenarios, while the row indicates the periods. The dotted points indicate areas with a 95 % confidence interval.

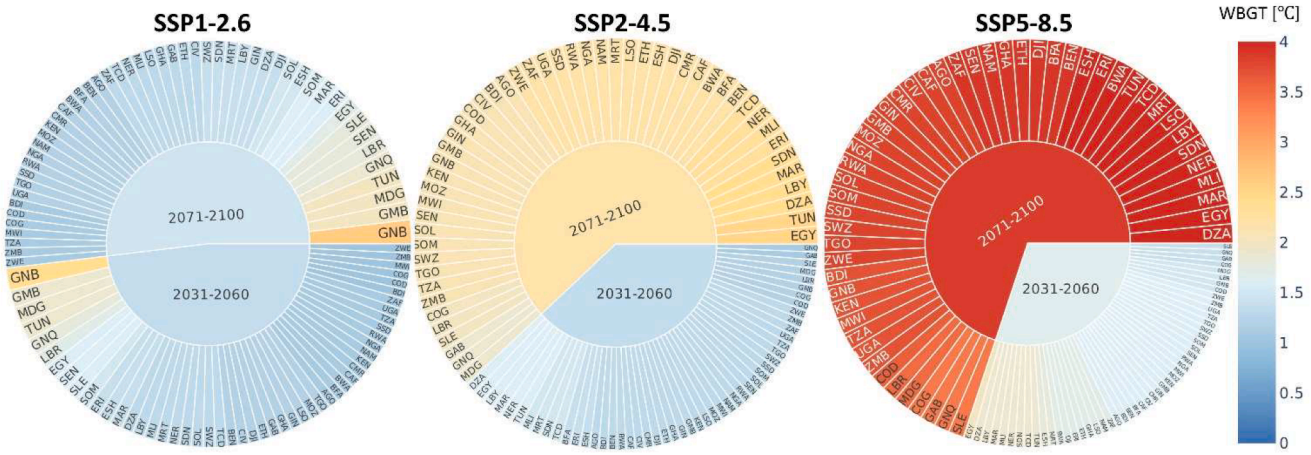

Fig. 6. 75th percentile projected changes in WBT across countries under different climate scenarios and periods of the multimodel ensemble mean of the NEX-GDDP-CMIP6. The countries are ranked in ascending order for each period for a given scenario. The different colors of each country and period indicate the values depicted in the color bar.

comparable to those in other areas of the world. A study by Ullah et al. (2022) found an increase of about 6.0 °C toward the end of the century in the South-Asia region under the SSP5–8.5 scenario. Additionally, an increase in the WBGT index is projected by the end of the century and could be more pronounced under the RCP8.5 scenario in Europe (Casanueva et al., 2020). Our results are also similar to those of several previous studies in Africa using different metrics, such as heat stress and discomfort indices, for heat-related risks to the human body (Sawadogo et al., 2024; Dajuma et al., 2023; Fotso-Nguemo et al., 2023; Parkes et al., 2022; Iyakaremye et al., 2021). The projected increase in the WBGT across Africa may significantly affect outdoor activities such as football. As WBGT levels rise, the thermal stress experienced by athletes during training and competitions can profoundly affect performance, health, and safety and increase the risk of exertional heat injuries (Hosokawa et al., 2019, 2018). The players' performance in Afcon's games may weaken under climate change, and this weakness could be more pronounced at the end of the century.

3.2.2. *Projected changes in the WBGT across African countries*

The projected changes in the WBGT index among countries vary, and the values range from 1 to 4.3 °C (Fig. 6). There is an increase in the WBGT values from the "challenge to mitigations scenario" to the "challenge to adaptations scenario" for each country. For instance, under the SSP5–8.5 scenario, an average increase value of 3.8 °C for the aggregated countries is expected for the 2071–2100 period, while a 1.47 °C increase is expected under SSP1–2.6 for the same period. Moreover, each country shows high values in the late century for all climate scenarios. Zimbabwe (ZWE) indicates the lowest increase under SSP1–2.6, while Sierra Leone (SLE) has the lowest increase for both periods under SSP5–8.5. Climate change will likely increase the WBGT index values by 1.7–2.6 °C in some countries, such as Guinea-Bissau (GNB; 2.6 °C), The Gambia (GMB; 2.0 °C), Madagascar (MDG; 2.0 °C) and Egypt (EGY; 1.7 °C), under SSP1–2.6 for the 2071–2100 period. The latter country has a higher rank, with an increase in the WBGT of 2.5 °C for 2071–2100 under the SSP2–4.5 scenario. Most of the northern African and Sahelian countries are among the ranked countries with the increase in the WBGT index under the SSP5–8.5 scenario. EGY (2.0 °C), followed by Algeria (DZA; 1.9 °C), has the highest increase for the near future, while in the far future, both countries have the same values of 4.3 °C. Overall, these findings suggest that Northern and Sahelian countries may experience a more pronounced increase in the WBGT index.

3.2.3. *Model agreement*

Fig. 7 illustrates the model spread of the projected changes in the WBGT index over each subregion. There is a high level of agreement among the models in terms of the projected changes in the WBGT over the different subregions. All the models exhibit a consistent increase in the WBGT in the near and far future and under the SSP scenarios. The projected minimum value of the WBGT among the models is greater than 0 for all periods and SSPs. This implies the robustness of the projected

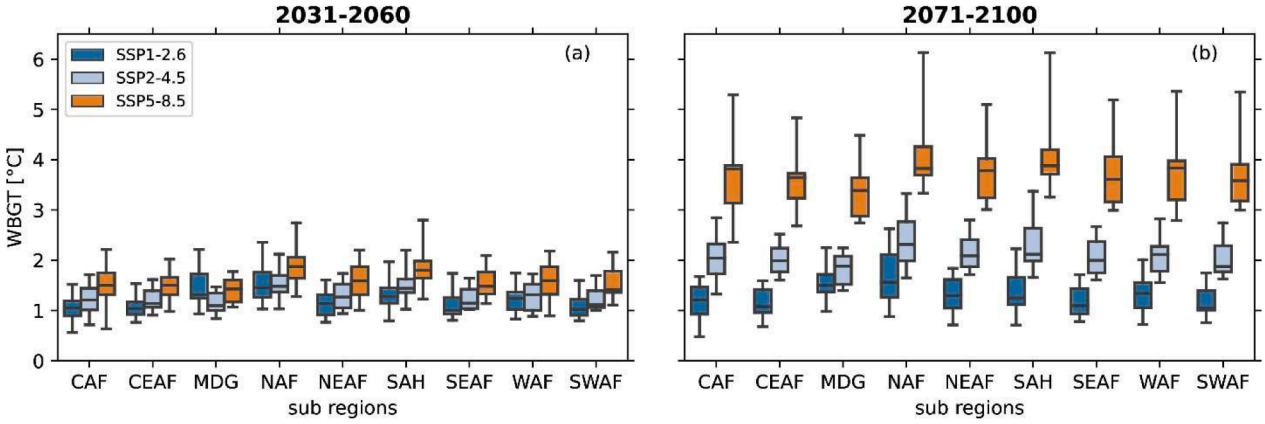

Fig. 7. Boxplot of the NEX-GDDP-CMIP6 models for the projected changes in the WBGT index over different subregions in Africa and for each climate change scenario: SSP1–2.6, SSP2–4.5 and SSP5–8.5. Panel (a) presents the near-future projections (2031–2060), while panel (b) illustrates the far-future projections (2071–2100).

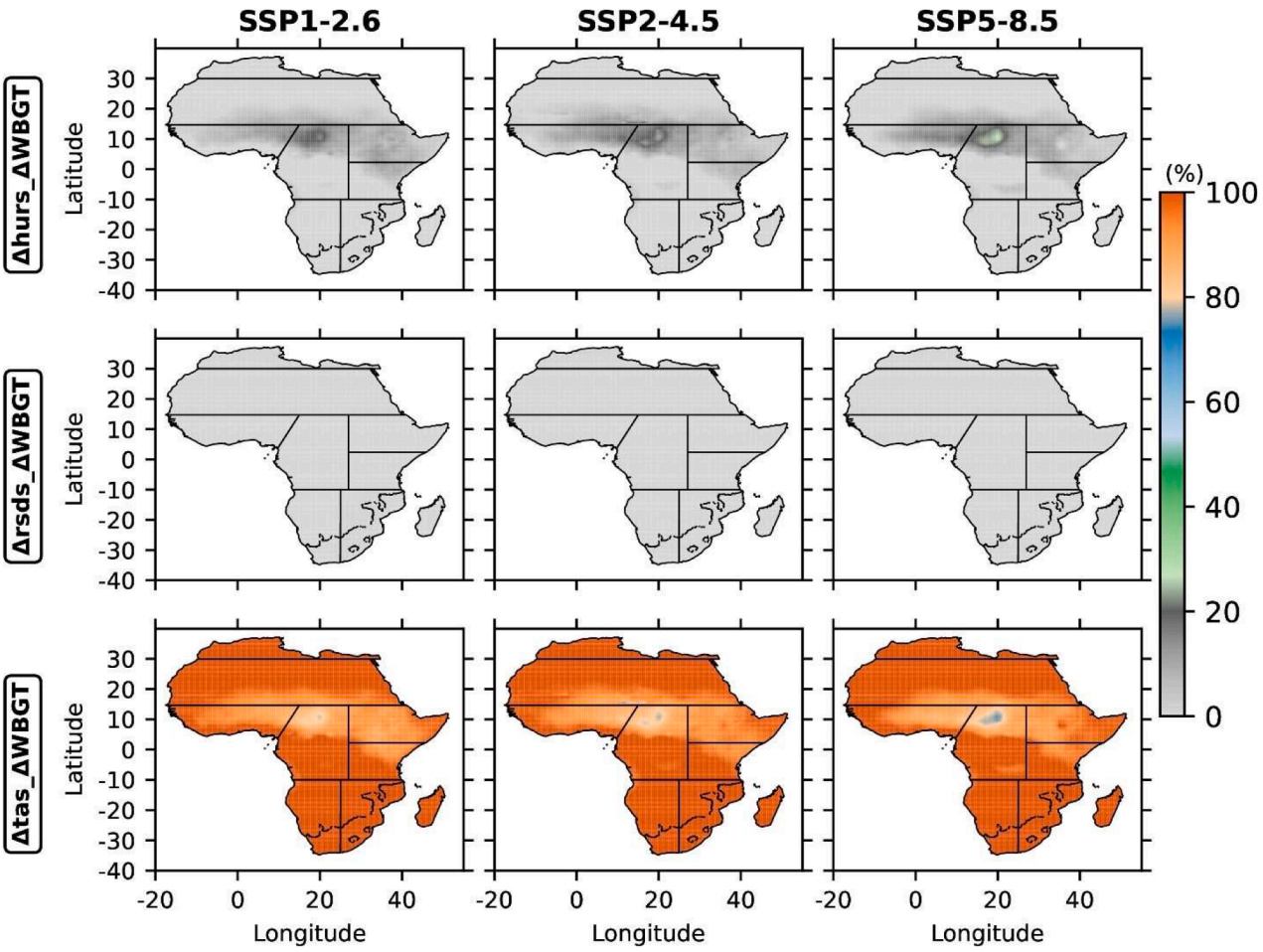

Fig. 8. Annual projected changes in the spatial distribution of the total change in the WBGT index of the multimodel ensemble mean of the NEX-GDDP-CMIP6 datasets due to the contributions of different variables across Africa under different climate scenarios in the near future (2031–2070). Δ*tas*_Δ*WBGT* indicates the contribution change in temperature (*tas*), while Δ*rsds*_Δ*WBGT* shows the contribution change in shortwave radiation (*rsds*). The contribution change in relative humidity (*hurs*) is illustrated by Δ*hurs*_Δ*WBGT*.

changes in the WBGT index in Africa. In addition, for all the subregions, the SSP5–8.5 scenario indicates the highest increase in both periods. Some subregions, such as the NAF and SAH, could experience an increase of approximately 6.0 °C under SSP5–8.5 in the far future, as shown by the maximum value projected by the model spread. However, there are some discrepancies in the increased magnitude of changes among the models. These discrepancies are stronger in the far future than in the near future. Moreover, the difference between each SSP is more pronounced in the 2071–2100 period compared to the 2031–2060 period for all subregions. This is the case in the WAF region, where the median difference between SSP5–8.5 and SSP1–2.6 is about 0.4 °C for the 2031–2060 period, while in the period of 2071–2100, it is about 2.5 °C. These findings reveal some uncertainties in the increase in the magnitude of the WBGT index over Africa, mainly due to the climate change scenario. Further discussions on these uncertainties will be provided in Section 3.2.6

3.2.4. Induced changes in the WBGT

The contribution of each variable involved in calculating the WBGT index is presented in Fig. 8 for the near future period and in Fig. 9 for the far future period. The total change in the WBGT index (Δ*WBGT*) due to the contribution of *tas* (Δ*tas*_Δ*WBGT*) indicates the largest contribution in all scenarios and time periods. Δtas_{WBGT} shows similar values across Africa of about 100 % except for some areas in the Sahelian Strip and Eastern Africa. In these areas, both Δ*tas*_Δ*WBGT* and Δ*hurs*_Δ*WBGT* contribute more to the increase in the WBGT. The projected changes in *hurs* show an increase over these areas but are much more pronounced in the far future than in the near future, with a value of 2.5 % (see FigS.1–2). This suggests that an increase in *hurs* could also contribute to Δ*WBGT* in Africa. However, the induced changes in Δ*hurs*_Δ*WBGT* and Δ*tas*_Δ*WBGT* are not consistent among scenarios and periods. Furthermore, in these localized areas, the contribution from *hurs* increases toward the highest scenario and to the later century. $\Delta hurs_{WBGT}$ is likely to increase by approximately 15 %, 30 %, and 40 % under the SSP1–2.6, SSP2–4.5, and SSP5–8.5 scenarios, respectively, in the near future in some areas of the Sahelian Strip and Eastern Africa. In the far future, $\Delta hurs_{WBGT}$ will contribute less than 20 % of these areas. Nonetheless, the contribution of *rsds* (Δ*rsds*_Δ*WBGT*) is negligible over the continent for each SSP scenario and period. This negligible effect of *rsds* on Δ*WBGT* could be attributed to the low relative change in the value of 5 $W.m^{-2}$ under climate change (see Fig. S1–2). These findings suggest that the increase in *tas* and *hurs* has a more substantial effect on the change in the WBGT index in Africa than the increase in *rsds*. Similar results were also found in China, where heat-related stress is more sensitive to the increase in temperature and humidity (Cheng et al., 2024).

3.2.5. Suitable countries

The projected changes in the WBGT index could contribute to the potential impacts of reduced player performance during the Afcon in a given host country. Fig. 10 shows the projected annual mean changes in the alert description status under the different SSPs and periods for each country. Most African countries may experience an escalation in alert

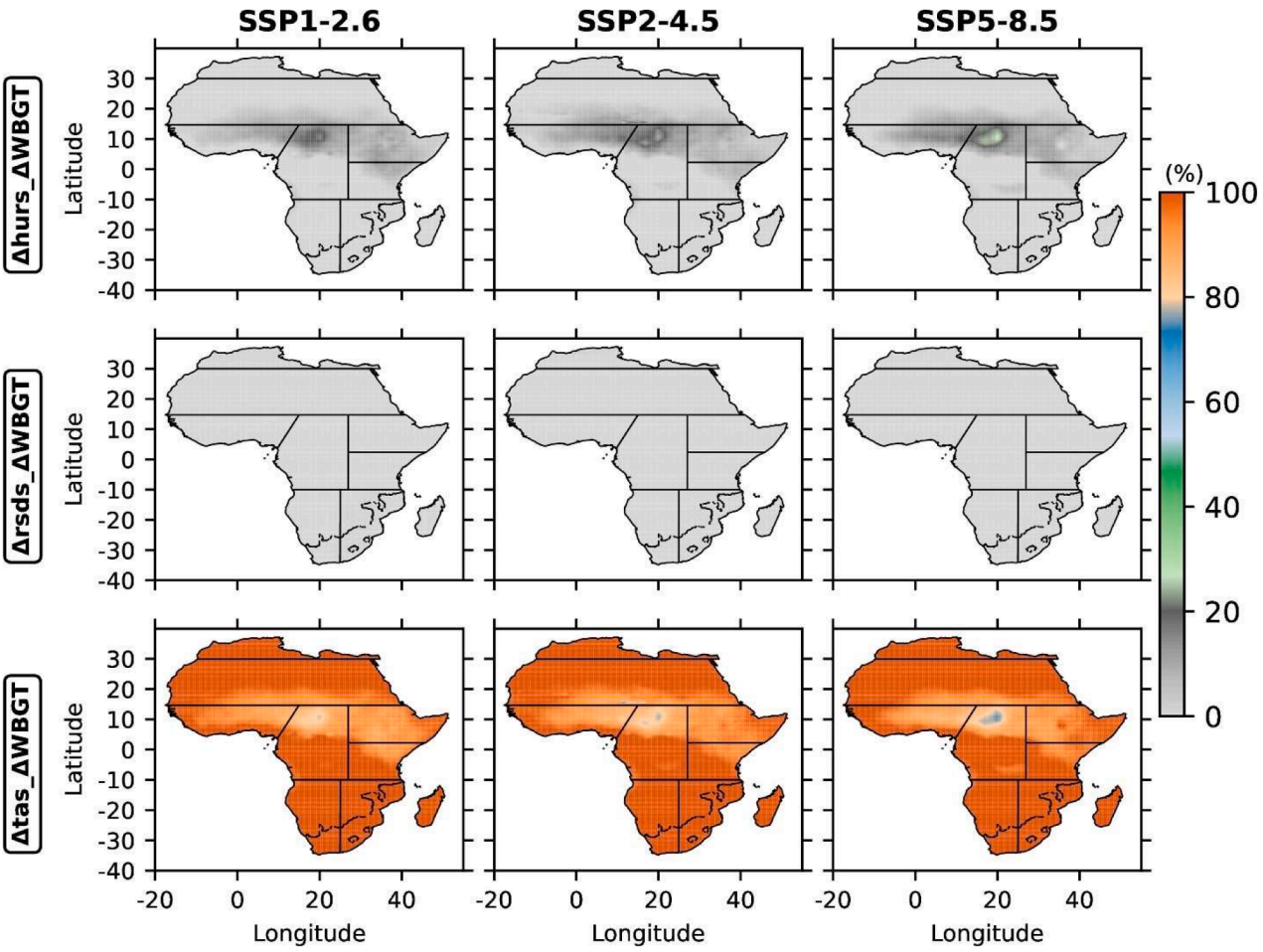

Fig. 9. Similar to Fig. 8 but for the far future (2071–2100).

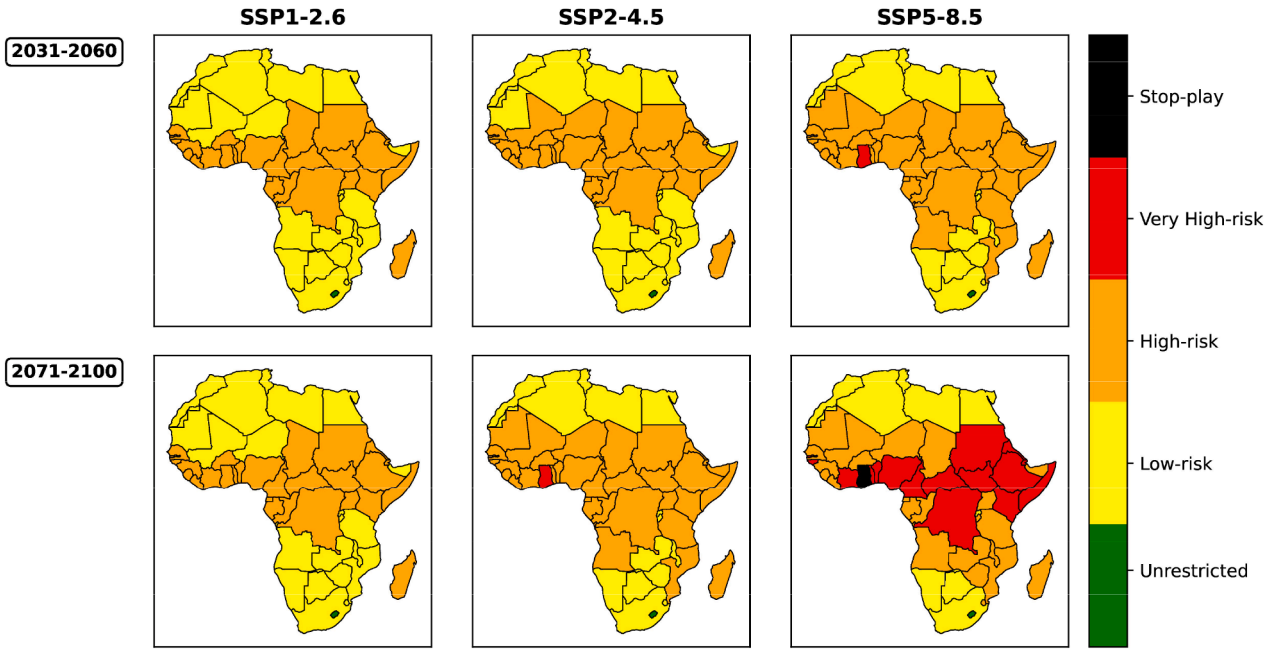

Fig. 10. Annual projected spatial distribution of the alert description status across African countries of the multimodel ensemble mean of the NEX-GDDP-CMIP6 (*EnsMean*) for different SSPs and periods. The color indicates the different warnings described in Table 1.

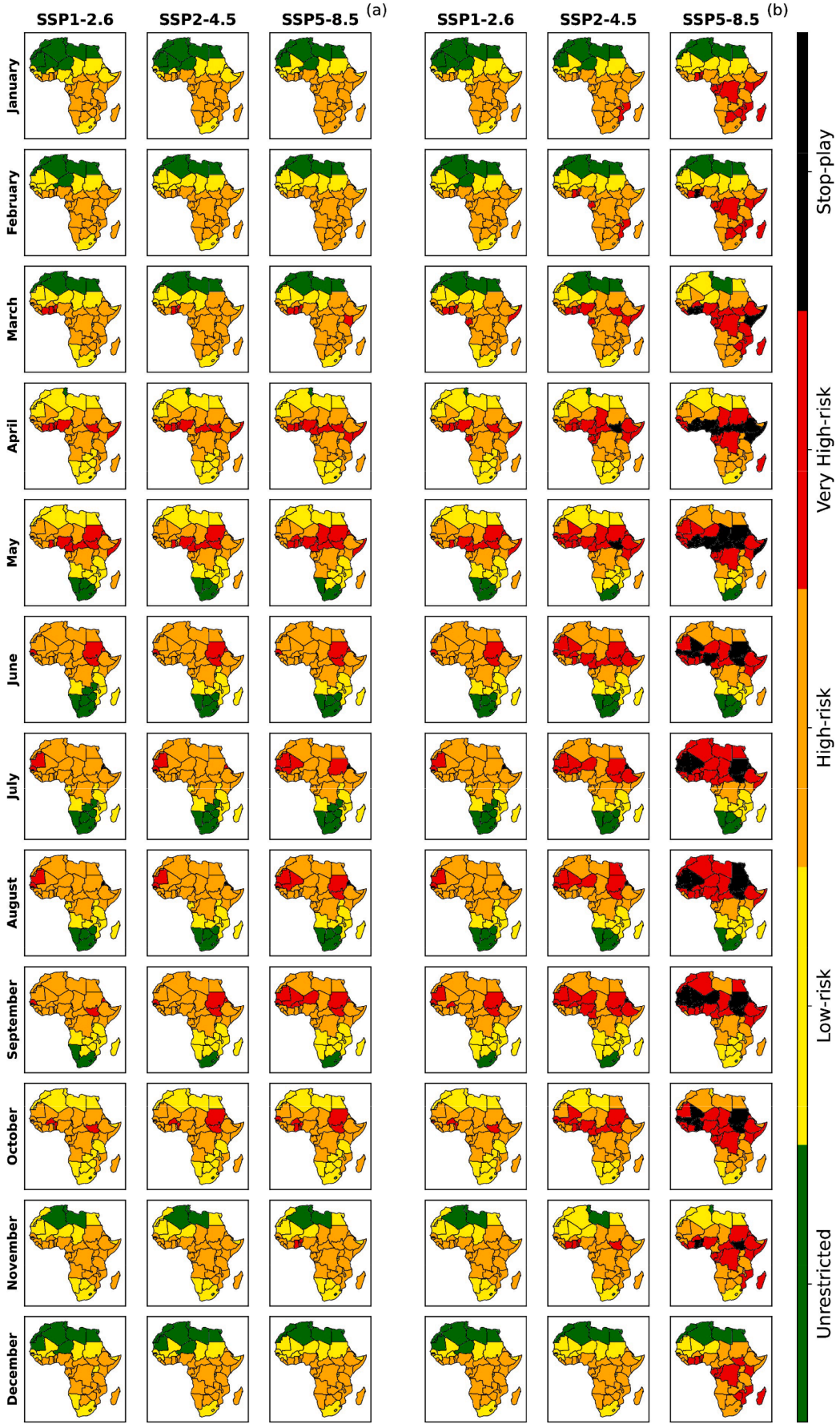

Fig. 11. Similar to Fig. 10 but on a monthly scale: (a) for the near future (2031–2060) and (b) for the far future (2071–2100).

description status under climate change. However, this escalation varies under different scenarios and over different periods. In the near future, several countries, such as Burkina Faso, Senegal, Guinea, Madagascar, and Uganda, may transition from low-risk to high-risk alert status under the SSP1–2.6 scenario. Libya and South Africa may lose their unrestricted alert status and shift to a low-risk alert status. The projected increase in the WBGT index will not impact the alert description status for the 2071–2100 period compared to that for the 2031–2060 period under SSP1–2.6. This is not true for the SSP2–4.5 scenario, where Ghana may shift from a high-risk alert status in the 2031–2100 period to a very high-risk alert status in the 2071–2100 period. The warning alert level of this country worsens, reaching a higher alert level under the SSP5–8.5 and 2071–2100 period. This can be attributed to an increase in the WBGT of approximately 3.9 °C (see Fig. 6) and the fact that the country already holds a high-risk alert status under the reference climate. In the same period and scenario, countries such as Côte d'Ivoire, Benin, Togo, Nigeria, Cameroon, the Republic of Central Africa, South Sudan, Sudan, Kenya, Ethiopia, and the Democratic Republic of the Congo exhibit a very high-risk warning alert compared to the high-risk alert status found in their reference climate. Nonetheless, some countries could have the opportunity to safely host Afcon under SSP5–8.5. This is the case for Morocco, Algeria, Tunisia, Libya, Egypt, Western Sahara, South Africa, Namibia, and Botswana, where they have low-risk alert status descriptions. Only Lesotho maintains an unrestricted alert status under all the SSPs and periods.

Assessing the suitability of hosting the Afcon on an annual scale provides a broad overview of climate conditions under climate change. However, monthly projection assessments offer a deeper understanding of the future climate change that could impact player performance during the tournament. Fig. 11 illustrates the projected changes in alert status descriptions for each month under the different SSPs for the 2031–2060 and 2071–2100 periods. The analysis focuses on particular months when the Afcon takes place. This is usually about 30 games over two months, either in January-February or June-July.

The monthly projection of the alert description status varies across countries, SSPs, and periods, with an escalation in warning level status. In the January-February months, most of the northern countries, including Mali, Mauritania, Western Sahara, and Niger, may maintain unrestricted alert status under the SSP1–2.6 scenario in the near future. This could be related to the decrease in *hurs* in these countries, despite the increase in *tas* (see FigS5–6). However, there is an escalation alert from an unrestricted alert status to a low-risk or high-risk alert status under the SSP2–4.5 and SSP5–8.5 scenarios. In these months, most countries may experience a high-risk alert status under the SSP2–4.5 and SSP5–8.5 scenarios in the near future. In the far future, Ghana, Togo, the Benin Republic, Gabon, and Mozambique will likely get a very-high alert status under the SSP2–4.5 scenario in February. Along with these countries, some countries like Côte d'Ivoire, Madagascar, Zimbabwe, Botswana, the Democratic Republic of Congo, Congo Brazzaville, Somalia, and Kenya could shift to a very-high alert status under the SSP5–8.5 scenario in the 2071–2100 period. Among these countries, only Ghana will exhibit a stop-play alert status in February under the SSP5–8.5 scenario in the far future. Also, southern countries, including Madagascar, may move from low-risk/high-risk (reference climate) to high-risk/very high-risk under the SSP5–8.5 scenario and the 2071–2100 period. Central and Eastern countries could shift to high-risk and very high-risk status under the SSP2–4.5 and SSP5–8.5 scenarios and in the 2071–2100 period. Our findings suggest that playing the Afcon in January-February could suit the northern and Sahelian countries under climate change.

On the other hand, in comparison to January and February, June and July exhibit high warning alerts across countries under all the SSPs and periods. The projected *EnsMean* shows an alert status escalation compared to most countries' reference climate. For instance, in June, Morrocco, Algeria, Tunisia, Libya, and Egypt may transition from low-risk to high-risk status under all SSPs and periods for June. Some countries, such as Senegal, South Sudan, Sudan, Mauritania, and Mali, may shift to a very high-risk alert status under the SSP scenarios and in the near future for the June-July months. This could be due to the increase in temperature of approximately 4–7 °C in these countries (see Fig. S5–8). Southern countries may maintain the alert restrictions found in the reference climate under all the SSPs and periods. This could be related to the decrease in *hurs* (more than 4 %) under the SSP scenarios in the June-July months (see Fig. S5). However, many countries are projected to experience a stop-play alert status in the 2071–2100 period under the SSP5–8.5 scenario. Senegal, Mali, Burkina Faso, Niger, South Sudan, Sudan, Nigeria, and Mauritania are likely to shift to a stop-play alert status under the SSP5–8.5 scenario in the far future. Generally, countries above the equator indicate a high waning alert in hosting the Afcon competition. This indicates potential unsuitability for hosting Afcon in the 2071–2100 period. Nevertheless, South Africa, Botswana, Zambia, Mozambique, and Namibia are suitable countries for hosting Afcon under the SSPs in the far future for the June-July months.

The study suggests that both periods of playing the Afcon could limit many countries, mainly in Western, Central, and Eastern Africa, from hosting one of the most prestigious football tournaments on the continent. This could be due to the projected increase in *tas* and *hurs* in these countries (FigS5–6). These projected changes in *tas* and *hurs* also align with previous studies on the continent (Almazroui et al., 2020; Brouillet & Joussaume, 2019). Our findings indicate that the January-February and June-July periods are suitable for hosting Afcon only in northern, Sahelian countries and southern countries, respectively. Therefore, climate change may prevent some Central, Western, and Eastern countries from hosting the Afcon under the SSP5–8.5 scenario. Our results support the Sustainable Development Goals (SDGs), especially SDG 13, highlighting a call for climate action, as the SSP5–8.5 scenario foci the increasing difficulty of hosting safe events in a warming climate. This emphasizes the need for low-emission pathways to mitigate the risks of extreme heat.

In addition, our findings extend not only to the Afcon tournament but also to the national football championship. Various countries in West and Central Africa show a high-risk alert status, and most of the months in their present climate could escalate to very high-risk or stop-play alert status. For instance, it may be challenging for countries such as Burkina Faso to play their national football championship from March to November under the SSP5–8.5 scenario and in the 2071–2100 period. In addition, it could be challenging for most northern countries to play football games between May and October under the SSP5–8.5 scenario and in the far future. The results demonstrate that an increase in the WBGT in Africa could also impact the national football championship, which is already affected by the need for well-designed stadiums. The future impacts of global warming on sports events in Africa underline the importance of climate-adapted urban planning for African cities. Encouraging the National Football Association to invest in sustainable design and cooling stadiums, which aligns with SDG 11. Recent studies have explored climate adaptation and resilience under extreme heat in urban settings, emphasizing public health measures and adaptable infrastructure to combat heat impacts (Kim & Kang, 2023; Anand et al., 2021; Mao et al., 2021; Ramyar et al., 2019). For instance, Kim and Kang (2023) demonstrated the effectiveness of targeted cooling interventions in urban centers, which could benefit high-exposure settings like Afcon, where outdoor activities are susceptible to heat risks. Likewise, Gollagher and Fastenrath (2023) analyzed how urban sports events could adopt heat mitigation strategies, underscoring the need for climate-sensitive approaches to protect participants and spectators.

3.2.6. Source of uncertainties in the projected change in the WBGT

Fig. 12 shows the contributions of uncertainty for the WBGT index quantified by the proportion of variance over Africa and its subregions. Most subregions show a similar contribution trend from the three uncertainty sources. In the short-term projection, the model uncertainty emerges as the highest source of uncertainty over Africa and its

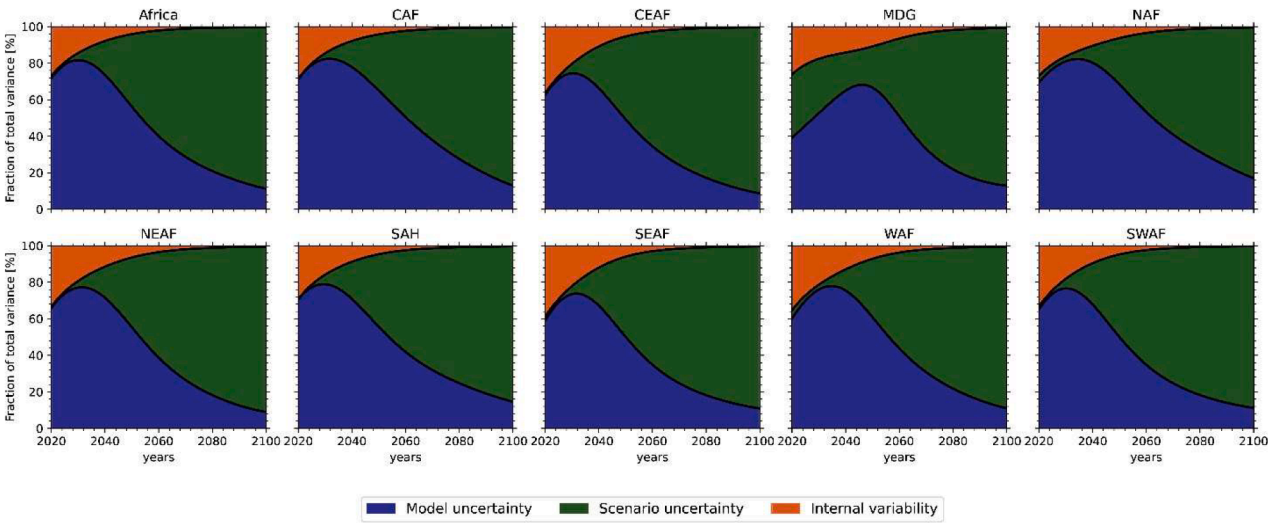

Fig. 12. Variance decomposition of the annual mean of the WBGT index into different uncertainty sources of the multimodel ensemble mean of the NEX-GDDP-CMIP6 datasets (blue: model uncertainty, green: scenario uncertainty, and orange: internal variability) over Africa and its subregions.

subregions at approximately 76.0 % of its peak. Moreover, the internal variability could contribute to about 33.25 % of the total in 2020 and decrease from 2026 to the end of the century. Additionally, in the short term, the contribution from climate scenarios is low compared to the uncertainty from the model and internal variability. This suggests that any SSPs can be used to project the impacts of WBGT in Africa in the short-term because there is not much difference in the magnitude of changes. Furthermore, the projected change in the WBGT in the short term should be carried out using the multimodel ensemble mean. However, in the long-term, significant uncertainties arise in the magnitude of the WBGT index under the SSP scenarios. This implies that in the long term (from the middle to the end of the century), scenario uncertainties could strongly contribute to the magnitude of changes in the WBGT index, as shown in Fig. 7-b. These insights suggest that climatological data may provide useful information for decision-making in the short-term projection of the WBGT. In contrast, in a long-term projection, multimodel and scenario spreads should be considered to address the escalating WBGT in Africa.

An athlete's physiological responses during physical exercise are significantly impacted by hot environmental conditions, influencing his or her performance (Drust et al., 2007). Global warming could negatively affect the environmental conditions in Africa, which is considered one of the hotspots of climate change. Some African countries may face challenges in hosting the Afcon tournament. The increase in temperature associated with relative humidity across these countries could affect the players' performance during the tournament. This could be similar to or worse than what was observed for the negative effects of high temperatures on players in the 2014 FIFA World Cup in Brazil (Chmura et al., 2017). With the projected changes in the WBGT over the African continent, players may be exposed to a hot environment during the Afcon tournament. They could face challenges in showcasing their skills. High temperatures during football games can reduce the intensity of exercise, sprint numbers, and total distance covered at high intensity and can impact the game's outcome (Nassis et al., 2015; Mohr et al., 2010). Nassis et al. (2015) showed that under high WBGT values, the number of passes was significantly impacted compared to a low-stress environment during the 2014 FIFA World Cup. Drust et al. (2005) reported that repeated maximal effort in a football game decreases the player's power under hot environmental conditions. Moreover, Mohr and Krustrup (2013) highlighted that repeated countermovement jumps are reduced in warm environments at approximately 30 °C after playing a football game. These could reduce the players' performance and pose a serious problem in the game. Despite these challenges, indicators such as the number of sprints, total distance covered, and power ability remain essential in assessing a football player's technical skills (Faude et al., 2012). However, our results suggest that the projected escalation in alert status across countries to high-risk, very high-risk, or stop-play alert status could lower the game quality in the Afcon tournament. Nonetheless, the number of shots, rate of successful passes, ball possession, number of goals, and number of cards may not be impacted despite the increase in WBGT (Illmer & Daumann, 2022).

Additionally, previous studies have shown that a high WBGT index is correlated with heat-related illness (Lewandowski et al., 2022; Spangler et al., 2022; Grundstein et al., 2012). Consequently, this can increase the risk of heat-related illnesses such as heat exhaustion and heatstroke. For instance, in the Afcon 2022 in Cameroon, a referee experienced a heatstroke during the Mali-Tunisia match. This incident underscores the importance of real-time monitoring of players and referees during a football game under high temperature and humidity. In response to such events, the CAF must implement robust health protocols to ensure safe conditions, such as cooling break time, acclimatization, light shirts, and strict application of heat-related stress protocols, aligning with SDG 3 on health and well-being. Also, natural grass on sports stadiums should be promoted over artificial turf surfaces, as they significantly absorb more heat and lead to higher WBGT levels, exposing players to high heat stress (Liu & Jim, 2021). Furthermore, rescheduling matches are essential under hot environmental conditions. This has been applied in the FIFA World Cup 2022 in Qatar, where the competition was shifted to late fall (November-December) due to hot environmental conditions (Sanderson, 2022).

However, it is essential to acknowledge that the suitability of hosting the Afcon tournament depends on a combination of factors beyond environmental conditions. For instance, infrastructure, logistics, approved stadiums, security, and safety are also included as criteria for hosting Afcon. Therefore, appropriate measures must be implemented to ensure the continued success of the Afcon in the face of challenging environmental conditions. Overall, our findings recommend that the organizers of Afcon need to consider the climatology data of the WBGT index of the host country and the future impacts of climate to reschedule the Afcon matches at appropriate months for the safety of players.

4. Summary and conclusion

This study investigated the potential impacts of climate change on the WBGT index over Africa and its subregions. The projected changes in the WBGT are used as a proxy to identify suitable countries for hosting

Afcon under climate change. We used eleven climate models from the NEX-GDDP-CMIP6, which were statistically downscaled to a spatial resolution of 25 km. Two datasets from ERA5 and SARAH-3 were used for the model evaluation. Three climate scenarios were used in this study: SSP1–2.6, SSP2–4.5, and SSP5–8.5. The projection changes are carried out in the near future (2031–2060) and far future (2071–2100) relative to the baseline period of 1985–2014. Moreover, this study investigated the potential contributions of *tas, hurs*, and *rsds* to the total change in WBGT in Africa. We also investigated the uncertainties related to future changes in the WBGT index. The analysis used the multimodel ensemble mean of the NEX-GDDP-CMIP6 datasets. The insights from this study can be summarized as follows:

- The ensemble mean relatively well captures the spatial distribution of the reference data for the WBGT index and related variables over Africa, with some biases.
- The ensemble mean projects a significant increase in the WBGT index under all SSPs and periods, with a pronounced increase under the SSP5–8.5 scenario and in the late century.
- Hosting the Afcon tournament could be a challenge for some countries under climate change, and this could require the CAF to reschedule the Afcon matches in appropriate months for the safety of players.
- The increases in *tas* and *hurs* are the main meteorological variables contributing to the future increase in the WBGT index in Africa. Moreover, this increase is associated with large uncertainties from climate scenarios, mainly long-term projections.

The projected changes in the WBGT index in Africa could put the Afcon tournament in danger, typically in January-February or June-July. The SSP1–2.6 shows more moderate increases in WBGT, suggesting that low-emission pathways could help preserve hosting viability for a broader range of countries. Our results highlight the importance of considering climate and weather information for decision-making when attributing the Afcon to a country. However, African countries could adopt environmental design strategies such as urban greening and shaded areas for climate change adaptation and mitigation to enhance microclimatic conditions. Such measures could make a tangible difference, especially in countries predicted to experience higher WBGT values (Niwa & Manabe, 2024), aligning with SDG 3 (Good Health and Well-being) and SDG 13 (Climate Action) for sustainable cities and societies.

Despite the valuable information in this study, there is still room for improvement. The use of daily data to compute the WBGT index could substantially underestimate its value during a particular day. For instance, Hosokawa et al. (2018) used sub-daily data to investigate the impacts of the WBGT index on players during the 2020 Olympic football tournament in Yokohama and Saitama, Japan. They found that 40–50 % of matches scheduled in the late morning and early afternoon exceeded the 30 °C WBGT index value. Using sub-daily data in the WBGT index at the time of playing at different group stages could provide more information on heat-related stress on players. Future research could expand on this work by exploring adjustments in event timing and infrastructure improvements to accommodate the changing climate. Moreover, accurate weather monitoring before a game could also offer safety to players. Advanced technologies like thermal imaging combined with artificial intelligence could be used for reliable estimation of the WBGT index in a stadium for heat stress assessment on players and spectators (Mahgoub et al., 2020). The CAF should also work with the host country's national meteorological agency and experts to provide an operational forecast for the WBGT index. In addition, different heat-related stresses, such as the universal thermal climate index and effective temperature, could be used to extend the knowledge on the impacts of heat-related stress on football players since the WBGT index has some limitations (Budd, 2008). Nonetheless, this study provides a benchmark for the impacts of climate change on the Afcon tournament, especially on potential host countries, and highlights the need to redesign major sports events under climate change.

Funding

This research is part of the WASCAL CONCERT, funded by the German Federal Ministry of Education and Research (BMBF). Funding reference number: 01LG2089A.

CRediT authorship contribution statement

Windmanagda Sawadogo: Writing – original draft, Visualization, Validation, Software, Methodology, Investigation, Formal analysis, Conceptualization. **Jan Bliefernicht:** Writing – review & editing, Visualization, Validation, Methodology. **Aissatou Faye:** Writing – review & editing, Visualization, Validation, Methodology. **Harald Kunstmann:** Writing – review & editing, Validation, Supervision, Project administration.

Declaration of competing interest

The authors declare that they have no known competing financial interests or personal relationships that could have influenced the work in this article.

Acknowledgments

We thank the European Centre for Medium-Range Weather Forecasts (ECMWF) for the ERA5 reanalysis and Satellite Application Facility on Climate Monitoring for providing the GHI data from SARAH-3. We are grateful to the Center for Climate Simulation for providing the NEX-GDDP-CMIP6 datasets. The authors would like to thank the anonymous reviewers for their valuable inputs in this manuscript.

Supplementary materials

Supplementary material associated with this article can be found, in the online version, at doi:10.1016/j.scs.2024.106091.

Data availability

The NEX-GDDP-CMIP6 can be downloaded via the NASA Center for Climate Simulation platform (https://nex-gddp-cmip6.s3.us-west-2.amazonaws.com/index.html#NEX-GDDP-CMIP6/). The ERA5 reanalysis data can be retrieved via the Copernicus platform (https://cds.climate.copernicus.eu/datasets/reanalysis-era5-single-levels?tab=overview). SARAH-3 can be retrieved via their platform (https://wui.cmsaf.eu/safira/action/viewProduktDetails?eid=22199_22482&fid=36). The data used in this study are available online.

References

Airiken, M., Li, S., Abulaiti, A., Wang, Y., & Zhang, L. (2023). Prediction of extreme climate on the Tibetan Plateau based on NEX-GDDP-CMIP6. *Human and Ecological Risk Assessment: An International Journal, 29*(9–10), 1261–1275. https://doi.org/10.1080/10807039.2023.2260493

Alduchov, O. A., & Eskridge, R. E. (1996). Improved Magnus form approximation of saturation vapor pressure. *Journal of Applied Meteorology, 35*(4), 601–609. https://doi.org/10.1175/1520-0450(1996)035<0601:IMFAOS>2.0.CO;2

Almazroui, M., Saeed, F., Saeed, S., Nazrul Islam, M., Ismail, M., Klutse, N. A. B., & Siddiqui, M. H. (2020). Projected change in temperature and precipitation over Africa from CMIP6. *Earth Systems and Environment, 4*(3), 455–475. https://doi.org/10.1007/s41748-020-00161-x

Anand, J., Sailor, D. J., & Baniassadi, A. (2021). The relative role of solar reflectance and thermal emittance for passive daytime radiative cooling technologies applied to rooftops. *Sustainable Cities and Society, 65*, Article 102612. https://doi.org/10.1016/j.scs.2020.102612

Austin, A. B., Collins, S. M., Huggins, R. A., Smith, B. A., & Bowman, T. G. (2021). The impact of environmental conditions on player loads during preseason training

sessions in women's soccer athletes. *The Journal of Strength & Conditioning Research, 35*(10), 2775. https://doi.org/10.1519/JSC.0000000000004112
Bitencourt, D. P., Muniz Alves, L., Shibuya, E. K., de Ângelo da Cunha, I., & Estevam de Souza, J. P. (2021). Climate change impacts on heat stress in Brazil—Past, present, and future implications for occupational heat exposure. *International Journal of Climatology, 41*(S1), E2741–E2756. https://doi.org/10.1002/joc.6877
Brimicombe, C., Wieser, K., Monthaler, T., Jackson, D., Bont, J. D., Chersich, M. F., & Otto, I. M. (2024). Effects of ambient heat exposure on risk of all-cause mortality in children younger than 5 years in Africa: A pooled time-series analysis. *The Lancet Planetary Health, 8*(9), e640–e646. https://doi.org/10.1016/S2542-5196(24)00160-8
Brocherie, F., & Millet, G. P. (2015). Is the Wet-Bulb Globe Temperature (WBGT) index relevant for exercise in the heat? *Sports Medicine, 45*(11), 1619–1621. https://doi.org/10.1007/s40279-015-0386-8
Brouillet, A., & Joussaume, S. (2019). Investigating the role of the relative humidity in the co-occurrence of temperature and heat stress extremes in CMIP5 projections. *Geophysical Research Letters, 46*(20), 11435–11443.
Budd, G. M. (2008). Wet-bulb globe temperature (WBGT)—Its history and its limitations. *Journal of Science and Medicine in Sport, 11*(1), 20–32. https://doi.org/10.1016/j.jsams.2007.07.003
CAF Technical Study Group: "TotalEnergies CAF AFCON Cote d'Ivoire 2023 has exceeded expectations on the field." (2024). https://www.cafonline.com/caf-africa-cup-of-nations/news/caf-technical-study-group-totalenergies-caf-afcon-cote-d-ivoire-2023-has-exceeded-expectations-on-the-field/.
Casanueva, A., Kotlarski, S., Fischer, A. M., Flouris, A. D., Kjellstrom, T., Lemke, B., Nybo, L., Schwierz, C., & Liniger, M. A. (2020). Escalating environmental summer heat exposure—A future threat for the European workforce. *Regional Environmental Change, 20*, 1–14.
Cheng, S., Wang, S., Li, M., & He, Y. (2024). Summer heatwaves in China during 1961–2021: The impact of humidity. *Atmospheric Research*, Article 107366.
Chmura, P., Konefał, M., Andrzejewski, M., Kosowski, J., Rokita, A., & Chmura, J. (2017). Physical activity profile of 2014 FIFA World Cup players, with regard to different ranges of air temperature and relative humidity. *International Journal of Biometeorology, 61*(4), 677–684. https://doi.org/10.1007/s00484-016-1245-5
Chmura, P., Liu, H., Andrzejewski, M., Chmura, J., Kowalczuk, E., Rokita, A., & Konefał, M. (2021). Is there meaningful influence from situational and environmental factors on the physical and technical activity of elite football players? Evidence from the data of 5 consecutive seasons of the German Bundesliga. *PLoS One, 16*(3), Article e0247771. https://doi.org/10.1371/journal.pone.0247771
Chowdhury, S., Hamada, Y., & Ahmed, K. S. (2017). Prediction and comparison of monthly indoor heat stress (WBGT and PHS) for RMG production spaces in Dhaka, Bangladesh. *Sustainable Cities and Society, 29*, 41–57. https://doi.org/10.1016/j.scs.2016.11.012
Dajuma, A., Sylla, M. B., Tall, M., Almazroui, M., Yassa, N., Diedhiou, A., & Giorgi, F. (2023). Projected expansion of hottest climate zones over Africa during the mid and late 21st century. *Environmental Research: Climate, 2*(2), Article 025002. https://doi.org/10.1088/2752-5295/acc08a
Das, P., Zhang, Z., Ghosh, S., Lu, J., Ayugi, B., Ojara, M. A., & Guo, X. (2023). Historical and projected changes in Extreme High Temperature events over East Africa and associated with meteorological conditions using CMIP6 models. *Global and Planetary Change, 222*, Article 104068. https://doi.org/10.1016/j.gloplacha.2023.104068
Drust, B., Atkinson, G., & Reilly, T. (2007). Future perspectives in the evaluation of the physiological demands of soccer. *Sports Medicine, 37*(9), 783–805. https://doi.org/10.2165/00007256-200737090-00003
Drust, B., Rasmussen, P., Mohr, M., Nielsen, B., & Nybo, L. (2005). Elevations in core and muscle temperature impairs repeated sprint performance. *Acta Physiologica Scandinavica, 183*(2), 181–190.
Ebi, K. L., Vanos, J., Baldwin, J. W., Bell, J. E., Hondula, D. M., Errett, N. A., Hayes, K., Reid, C. E., Saha, S., Spector, J., & Berry, P. (2021). Extreme weather and climate change: population health and health system implications. *Annual Review of Public Health, 42*, 293–315. https://doi.org/10.1146/annurev-publhealth-012420-105026. Volume 42, 2021.
ECMWF. (2024). *Warmest February on record, the 9th consecutive warmest month.* https://climate.copernicus.eu/warmest-february-record-9th-consecutive-warmest-month#:~:text=February%202024%20was%20the%20warmest,Climate%20Change%20Service%20(C3S).
Faude, O., Koch, T., & Meyer, T. (2012). Straight sprinting is the most frequent action in goal situations in professional football. *Journal of Sports Sciences, 30*(7), 625–631.
FIFA. (2015). *Football emergency medicine manual 2nd edition.* https://digitalhub.fifa.com/m/26f48cc2b5c24e6e/original/szriio9ble9hvoyns04h-pdf.pdf.
Fischer, E. M., Sedláček, J., Hawkins, E., & Knutti, R. (2014). Models agree on forced response pattern of precipitation and temperature extremes. *Geophysical Research Letters, 41*(23), 8554–8562. https://doi.org/10.1002/2014GL062018
Fotso-Nguemo, T. C., Weber, T., Diedhiou, A., Chouto, S., Vondou, D. A., Rechid, D., & Jacob, D. (2023). Projected impact of increased global warming on heat stress and exposed population over Africa. *Earth's Future, 11*(1), Article e2022EF003268. https://doi.org/10.1029/2022EF003268
Gibson, O. R., James, C. A., Mee, J. A., Willmott, A. G. B., Turner, G., Hayes, M., & Maxwell, N. S. (2019). Heat alleviation strategies for athletic performance: A review and practitioner guidelines. *Temperature: Multidisciplinary Biomedical Journal, 7*(1), 3–36. https://doi.org/10.1080/23328940.2019.1666624
Gollagher, P., & Fastenrath, S. (2023). Transformative climate resilience and sport mega-events – The case of the Australian Open. *Environmental Innovation and Societal Transitions, 48*, Article 100762. https://doi.org/10.1016/j.eist.2023.100762
Grantham, J., Cheung, S. S., Connes, P., Febbraio, M. A., Gaoua, N., González-Alonso, J., Hue, O., Johnson, J. M., Maughan, R. J., Meeusen, R., Nybo, L., Racinais, S., Shirreffs, S. M., & Dvorak, J. (2010). Current knowledge on playing football in hot environments. *Scandinavian Journal of Medicine & Science in Sports, 20*(3), 161–167. https://doi.org/10.1111/j.1600-0838.2010.01216.x. *Suppl.*
Grundstein, A. J., Ramseyer, C., Zhao, F., Pesses, J. L., Akers, P., Qureshi, A., Becker, L., Knox, J. A., & Petro, M. (2012). A retrospective analysis of American football hyperthermia deaths in the United States. *International Journal of Biometeorology, 56*, 11–20.
Hajizadeh, R., Farhang Dehghan, S., Golbabaei, F., Jafari, S. M., & Karajizadeh, M. (2017). Offering a model for estimating black globe temperature according to meteorological measurements. *Meteorological Applications, 24*(2), 303–307. https://doi.org/10.1002/met.1631
Hall, A., Horta, A., Khan, M. R., & Crabbe, R. A. (2022). Spatial analysis of outdoor wet bulb globe temperature under RCP4.5 and RCP8.5 scenarios for 2041–2080 across a range of temperate to hot climates. *Weather and Climate Extremes, 35*, Article 100420. https://doi.org/10.1016/j.wace.2022.100420
Hawkins, E., & Sutton, R. (2009). The potential to narrow uncertainty in regional climate predictions. *Bulletin of the American Meteorological Society, 90*(8), 1095–1108. https://doi.org/10.1175/2009BAMS2607.1
Hersbach, H., Bell, B., Berrisford, P., Hirahara, S., Horányi, A., Muñoz-Sabater, J., Nicolas, J., Peubey, C., Radu, R., Schepers, D., & others. (2020). The ERA5 global reanalysis. *Quarterly Journal of the Royal Meteorological Society, 146*(730), 1999–2049.
Hosokawa, Y., Casa, D. J., Trtanj, J. M., Belval, L. N., Deuster, P. A., Giltz, S. M., Grundstein, A. J., Hawkins, M. D., Huggins, R. A., Jacklitsch, B., Jardine, J. F., Jones, H., Kazman, J. B., Reynolds, M. E., Stearns, R. L., Vanos, J. K., Williams, A. L., & Williams, W. J. (2019). Activity modification in heat: Critical assessment of guidelines across athletic, occupational, and military settings in the USA. *International Journal of Biometeorology, 63*(3), 405–427. https://doi.org/10.1007/s00484-019-01673-6
Hosokawa, Y., Grundstein, A. J., & Casa, D. J. (2018). Extreme heat considerations in International Football Venues: The utility of climatologic data in decision making. *Journal of Athletic Training, 53*(9), 860–865. https://doi.org/10.4085/1062-6050-361-17
Illmer, S., & Daumann, F. (2022). The effects of weather factors and altitude on physical and technical performance in professional soccer: A systematic review. *JSAMS Plus, 1*, Article 100002.
Iyakaremye, V., Zeng, G., Yang, X., Zhang, G., Ullah, I., Gahigi, A., Vuguziga, F., Asfaw, T. G., & Ayugi, B. (2021). Increased high-temperature extremes and associated population exposure in Africa by the mid-21st century. *Science of The Total Environment, 790*, Article 148162.
Jerez, S., Tobin, I., Vautard, R., Montávez, J. P., López-Romero, J. M., Thais, F., Bartok, B., Christensen, O. B., Colette, A., Déqué, M., & others. (2015). The impact of climate change on photovoltaic power generation in Europe. *Nature Communications, 6*, 10014.
Kakaei, H., Omidi, F., Ghasemi, R., Sabet, M. R., & Golbabaei, F. (2019). Changes of WBGT as a heat stress index over the time: A systematic review and meta-analysis. *Urban Climate, 27*, 284–292. https://doi.org/10.1016/j.uclim.2018.12.009
Kim, J., & Kang, J. (2023). AI based temperature reduction effect model of fog cooling for human thermal comfort: Climate adaptation technology. *Sustainable Cities and Society, 95*, Article 104574. https://doi.org/10.1016/j.scs.2023.104574
Kong, Q., & Huber, M. (2022). Explicit calculations of wet-bulb globe temperature compared with approximations and why it matters for labor productivity. *Earth's Future, 10*(3), Article e2021EF002334.
Kyaw, A. K., Hamed, M. M., Kamruzzaman, M., & Shahid, S. (2023). Spatiotemporal changes in population exposure to heat stress in South Asia. *Sustainable Cities and Society, 93*, Article 104544. https://doi.org/10.1016/j.scs.2023.104544
Lewandowski, S. A., Kioumourtzoglou, M.-A., & Shaman, J. L. (2022). Heat stress illness outcomes and annual indices of outdoor heat at U.S. Army installations. *PLoS One, 17*(11), Article e0263803. https://doi.org/10.1371/journal.pone.0263803
Liu, Z., & Jim, C. Y. (2021). Playing on natural or artificial turf sports field? Assessing heat stress of children, young athletes, and adults in Hong Kong. *Sustainable Cities and Society, 75*, Article 103271. https://doi.org/10.1016/j.scs.2021.103271
Locke, J., Dsilva, J., & Zarmukhambetova, S. (2023). Decarbonization Strategies in the UAE Built Environment: An Evidence-Based Analysis Using COP26 and COP27 Recommendations. *Sustainability, 15*(15), Article 15. https://doi.org/10.3390/su151511603
Mahgoub, A. O., Gowid, S., & Ghani, S. (2020). Global evaluation of WBGT and SET indices for outdoor environments using thermal imaging and artificial neural networks. *Sustainable Cities and Society, 60*, Article 102182. https://doi.org/10.1016/j.scs.2020.102182
Mao, H., Meng, Q., Li, S., Qi, Q., Wang, S., & Wang, J. (2021). Cooling effects of a mist-spraying system on ethylene tetrafluoroethylene cushion roofs in hot-humid areas: A case study in Guangzhou, China. *Sustainable Cities and Society, 74*, Article 103211. https://doi.org/10.1016/j.scs.2021.103211
Maslin, M. A., Lang, J., & Harvey, F. (2023). A short history of the successes and failures of the international climate change negotiations. *UCL Open Environment, 5*. https://doi.org/10.14324/111.444/ucloe.000059
Mohr, M., & Krustrup, P. (2013). Heat stress impairs repeated jump ability after competitive elite soccer games. *The Journal of Strength & Conditioning Research, 27*(3), 683–689.
Mohr, M., Mujika, I., Santisteban, J., Randers, M. B., Bischoff, R., Solano, R., Hewitt, A., Zubillaga, A., Peltola, E., & Krustrup, P. (2010). Examination of fatigue development in elite soccer in a hot environment: A multi-experimental approach. *Scandinavian Journal of Medicine & Science in Sports, 20*, 125–132.

Mohr, M., Nybo, L., Grantham, J., & Racinais, S. (2012). Physiological Responses and Physical Performance during Football in the Heat. *PLoS One, 7*(6), e39202. https://doi.org/10.1371/journal.pone.0039202

Nassis, G. P., Brito, J., Dvorak, J., Chalabi, H., & Racinais, S. (2015). The association of environmental heat stress with performance: Analysis of the 2014 FIFA World Cup Brazil. *British Journal of Sports Medicine, 49*(9), 609–613. https://doi.org/10.1136/bjsports-2014-094449

Newth, D., & Gunasekera, D. (2018). Projected changes in wet-bulb globe temperature under alternative climate scenarios. *Atmosphere, 9*(5), Article 5. https://doi.org/10.3390/atmos9050187

Niwa, H., & Manabe, R. (2024). WBGT prediction with high spatial resolution using actual measurement data and data acquired using infrared sensors mounted on UAVs. *Sustainable Cities and Society, 107*, Article 105470. https://doi.org/10.1016/j.scs.2024.105470

Nyiwul, L. (2021). Climate change adaptation and inequality in Africa: Case of water, energy and food insecurity. *Journal of Cleaner Production, 278*, Article 123393. https://doi.org/10.1016/j.jclepro.2020.123393

O'Neill, B. C., Carter, T. R., Ebi, K., Harrison, P. A., Kemp-Benedict, E., Kok, K., Kriegler, E., Preston, B. L., Riahi, K., Sillmann, J., van Ruijven, B. J., van Vuuren, D., Carlisle, D., Conde, C., Fuglestvedt, J., Green, C., Hasegawa, T., Leininger, J., Monteith, S., & Pichs-Madruga, R. (2020). Achievements and needs for the climate change scenario framework. *Nature Climate Change, 10*(12), 1074–1084. https://doi.org/10.1038/s41558-020-00952-0

O'Neill, B. C., Kriegler, E., Riahi, K., Ebi, K. L., Hallegatte, S., Carter, T. R., Mathur, R., & van Vuuren, D. P. (2014). A new scenario framework for climate change research: The concept of shared socioeconomic pathways. *Climatic Change, 122*(3), 387–400. https://doi.org/10.1007/s10584-013-0905-2

Ozgünen, K. T., Kurdak, S. S., Maughan, R. J., Zeren, C., Korkmaz, S., Yazici, Z., Ersöz, G., Shirreffs, S. M., Binnet, M. S., & Dvorak, J. (2010). Effect of hot environmental conditions on physical activity patterns and temperature response of football players. *Scandinavian Journal of Medicine & Science in Sports, 20*(3), 140–147. https://doi.org/10.1111/j.1600-0838.2010.01219.x. *Suppl.*

Parkes, B., Buzan, J. R., & Huber, M. (2022). Heat stress in Africa under high intensity climate change. *International Journal of Biometeorology, 66*(8), 1531–1545. https://doi.org/10.1007/s00484-022-02295-1

Parsons, K. (2006). Heat stress standard ISO 7243 and its global application. *Industrial Health, 44*(3), 368–379. https://doi.org/10.2486/indhealth.44.368

Pfeifroth, U., Kothe, S., Drücke, J., Trentmann, J., Schröder, M., Selbach, N., & Hollmann, R. (2023). *Surface radiation data set—heliosat (SARAH)—Edition 3*. Satellite Application Facility on Climate Monitoring (CM SAF). https://doi.org/10.5676/EUM_SAF_CM/SARAH/V003

Racinais, S., Alonso, J. M., Coutts, A. J., Flouris, A. D., Girard, O., González-Alonso, J., Hausswirth, C., Jay, O., Lee, J. K. W., Mitchell, N., Nassis, G. P., Nybo, L., Pluim, B. M., Roelands, B., Sawka, M. N., Wingo, J. E., & Périard, J. D. (2015). Consensus recommendations on training and competing in the heat. *Scandinavian Journal of Medicine & Science in Sports, 25*(S1), 6–19. https://doi.org/10.1111/sms.12467

Raines, K., & Fitchett, J. M. (2024). Exploring the risk of heat stress in high school pre-season sports training, Johannesburg, South Africa. *International Journal of Biometeorology*. https://doi.org/10.1007/s00484-024-02748-9

Ramyar, R., Zarghami, E., & Bryant, M. (2019). Spatio-temporal planning of urban neighborhoods in the context of global climate change: Lessons for urban form design in Tehran, Iran. *Sustainable Cities and Society, 51*, Article 101554. https://doi.org/10.1016/j.scs.2019.101554

Rao, K. K., Al Mandous, A., Al Ebri, M., Al Hameli, N., Rakib, M., & Al Kaabi, S. (2024). Future changes in the precipitation regime over the Arabian Peninsula with special emphasis on UAE: Insights from NEX-GDDP CMIP6 model simulations. *Scientific Reports, 14*(1), 151. https://doi.org/10.1038/s41598-023-49910-8

Sanderson, K. (2022). How will World Cup footballers cope with Qatar heat? *Nature, 612*(7938), 19.

Sawadogo, W., Abiodun, B. J., & Okogbue, E. C. (2019). Impact of global warming on photovoltaic power generation over West Africa. *Renewable Energy*. https://doi.org/10.1016/j.renene.2019.11.032

Sawadogo, W., Bliefernicht, J., Fersch, B., Salack, S., Guug, S., Diallo, B., Ogunjobi, Kehinde. O., Nacoulma, G., Tanu, M., Meilinger, S., & Kunstmann, H. (2023). Hourly global horizontal irradiance over West Africa: A case study of one-year satellite- and reanalysis-derived estimates vs. In situ measurements. *Renewable Energy*. , Article 119066. https://doi.org/10.1016/j.renene.2023.119066

Sawadogo, W., Neya, T., Semde, I., Korahiré, J. A., Combasséré, A., Traoré, D. E., Ouedraogo, P., Diasso, U. J., Abiodun, B. J., Bliefernicht, J., & Kunstmann, H. (2024). Potential impacts of climate change on the Sudan-Sahel region in West Africa – Insights from Burkina Faso. *Environmental Challenges, 15*, Article 100860. https://doi.org/10.1016/j.envc.2024.100860

Sawadogo, W., Reboita, M. S., Faye, A., da Rocha, R. P., Odoulami, R. C., Olusegun, C. F., Adeniyi, M. O., Abiodun, B. J., Sylla, M. B., Diallo, I., Coppola, E., & Giorgi, F. (2020). Current and future potential of solar and wind energy over Africa using the RegCM4 CORDEX-CORE ensemble. *Climate Dynamics*. https://doi.org/10.1007/s00382-020-05377-1

Spangler, K. R., Liang, S., & Wellenius, G. A. (2022). Wet-bulb globe temperature, universal thermal climate index, and other heat metrics for US Counties, 2000–2020. *Scientific Data, 9*(1), 326. https://doi.org/10.1038/s41597-022-01405-3

Stull, R. (2011). Wet-bulb temperature from relative humidity and air temperature. *Journal of Applied Meteorology and Climatology, 50*(11), 2267–2269. https://doi.org/10.1175/JAMC-D-11-0143.1

Sylla, M. B., Faye, A., Giorgi, F., Diedhiou, A., & Kunstmann, H. (2018). Projected heat stress under 1.5°C and 2°C global warming scenarios creates unprecedented discomfort for humans in West Africa. *Earth's Future, 6*(7), 1029–1044. https://doi.org/10.1029/2018EF000873

Thrasher, B., Wang, W., Michaelis, A., Melton, F., Lee, T., & Nemani, R. (2022). NASA global daily downscaled projections, CMIP6. *Scientific Data, 9*(1), 262. https://doi.org/10.1038/s41597-022-01393-4

Tripp, B., Vincent, H. K., Bruner, M., & Smith, M. S. (2020). Comparison of wet bulb globe temperature measured on-site vs estimated and the impact on activity modification in high school football. *International Journal of Biometeorology, 64*(4), 593–600. https://doi.org/10.1007/s00484-019-01847-2

Ullah, I., Saleem, F., Iyakaremye, V., Yin, J., Ma, X., Syed, S., Hina, S., Asfaw, T. G., & Omer, A. (2022). Projected changes in socioeconomic exposure to heatwaves in South Asia under changing climate. *Earth's Future, 10*(2), Article e2021EF002240.

UNFCCC. (1992). *United Nations Framework Convention on Climate Change*. https://unfccc.int/resource/docs/convkp/conveng.pdf.

Vicedo-Cabrera, A. M., Scovronick, N., Sera, F., Royé, D., Schneider, R., Tobias, A., Astrom, C., Guo, Y., Honda, Y., Hondula, D. M., Abrutzky, R., Tong, S., Coelho, M., de, S. Z. S., Saldiva, P. H. N., Lavigne, E., Correa, P. M., Ortega, N. V., Kan, H., Osorio, S., … Gasparrini, A. (2021). The burden of heat-related mortality attributable to recent human-induced climate change. *Nature Climate Change, 11*(6), 492–500. https://doi.org/10.1038/s41558-021-01058-x

Warner, K., & van der Geest, K. (2013). Loss and damage from climate change: Local-level evidence from nine vulnerable countries. *International Journal of Global Warming, 5*(4), 367–386. https://doi.org/10.1504/IJGW.2013.057289

Yengoh, G. T., & Ardö, J. (2020). Climate Change and the future heat stress challenges among smallholder farmers in East Africa. *Atmosphere, 11*(7), Article 7. https://doi.org/10.3390/atmos11070753

Zare, S., Hasheminejad, N., Shirvan, H. E., Hemmatjo, R., Sarebanzadeh, K., & Ahmadi, S. (2018). Comparing Universal Thermal Climate Index (UTCI) with selected thermal indices/environmental parameters during 12 months of the year. *Weather and Climate Extremes, 19*, 49–57. https://doi.org/10.1016/j.wace.2018.01.004